Infrared spectroelectrochemistry

ARTICLE *in* CHEMICAL REVIEWS · APRIL 1988

Impact Factor: 46.57 · DOI: 10.1021/cr00086a006

Infrared Spectroelectrochemistry

KEVIN ASHLEY

Department of Chemistry, San Jose State University, San Jose, California 95192

STANLEY PONS*

Department of Chemistry, University of Utah, Salt Lake City, Utah 84112

Received November 4, 1987 (Revised Manuscript Received March 28, 1988)

Contents

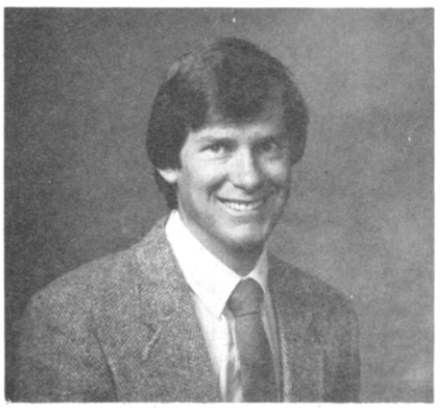

Kevin Ashley is Assistant Professor of Chemistry at San Jose State University. He was born near Chicago in 1958 and was raised in Arizona. He received a B.S. degree in Biology from the University of Arizona in 1980. After a year with the Arizona Bureau of Geology and Mineral Technology (Geothermal Group), he enrolled at Northern Arizona University, where he received an M.S. in Chemistry in 1984. Subsequently he joined Stanley Pons' research group at the University of Utah, where he completed his Ph.D. in 1987. Dr. Ashley then joined the chemistry faculty at San Jose State in January 1988. His research interests include conducting polymers, chemistry at interfaces, battery electrochemistry, and bioelectrochemistry.

Stanley Pons is a Professor of Chemistry at the University of Utah. A native of North Carolina, he obtained his B.S. at Wake Forest University, and attended graduate school at the University of Michigan (H. B. Mark, Jr.). In 1967, he went into private business until returning to graduate school at Southampton. He obtained his Ph.D. (Alan Bewick) in 1979. He was on the faculties of Oakland University and the University of Alberta before joining Utah in 1983. Professor Pons' research interests have been in the areas of spectroelectrochemistry and microelectrodes and their application to a wide variety of electrochemical problems. He has published over 135 research papers and one book.

I. Introduction

The primary focus of studies of the electrode–solution interface using in situ methods is the characterization at the molecular level of adsorbed species, species in the electrical double layer, and species in the reaction–diffusion layer near the electrode surface. Additionally, the results of the very sensitive electron spectroscopic, electron diffraction, and imaging techniques for the metal–high-vacuum and metal–ultrahigh-vacuum systems have provided detailed information regarding

0009-2665/88/0788-0673$06.50/0

those systems. These techniques include low-energy electron diffraction spectroscopy (LEED), Auger electron spectroscopy (AES), electron energy loss spectroscopy (EELS), ultraviolet photoelectron spectroscopy (UPS), ion-scattering spectroscopy, scanning electron spectroscopy, inelastic electron tunneling (IETS), transmission electron diffraction microscopy, reflection high-energy electron diffraction (RHEED), X-ray photoelectron spectroscopy (XPS), and secondary ion mass spectroscopy (SIMS). While these techniques have recently been applied to problems of electrochemical interest,[1-3] the spectroscopy must be performed external to the electrochemical experiment. Typically, adsorption of a species or surface modification is accomplished by an electrochemical technique at a metal substrate, and the modified surface is transported from the reaction solution to a high-vacuum probe for analysis. The question of preservation of the adsorbate structure when a transfer between such radically different environments is made has not been totally resolved. At room temperature, high-vacuum experiments are best suited to the study of strongly adsorbed (chemisorbed) species. In situ interfacial probes, including the Raman spectroscopies, infrared spectroscopy, infrared reflection–absorption spectroscopy, UV–visible techniques, Mössbauer spectroscopy, SEXAFS, and X-ray diffraction, can also provide information on weakly adsorbed species. With these techniques, we seek information regarding the energetics and identification of species in the interface, as well as determination of long- and short-range order. The methods are limited, however, to absorption, diffraction, or scattering of only a few types of fundamental particles. Infrared spectroelectrochemical techniques, including polarization modulation techniques, have been developed to such a level that it is now possible to observe surface energetic changes spectroscopically as a function of the reaction driving force. Vibrational spectroscopy is particularly well suited to these studies since it becomes possible to obtain both speciation information and information regarding the environment around the species of interest. Inferences can be made regarding adsorbate orientation, identification of intermediates and products, catalytic and other reaction mechanisms, and the influence of electromagnetic fields on molecules.

Early efforts in electrochemical vibrational spectroscopy[4-6] were based on the use of optically transparent electrodes (OTEs). These were typically infrared transparent germanium plate electrodes or thin metal films deposited on an infrared transparent substrate and were used as internal reflectance elements. These experiments were limited in sensitivity, and the restricted choice of infrared transparent electrode materials was also a disadvantage. Many of the problems associated in obtaining vibrational spectra of surface species are eliminated by the use of external reflection cells. The first such experiments using them were for obtaining Raman spectra of electrochemical systems[7] (these efforts led to the discovery of surface-enhanced Raman spectroscopy[8] (SERS)). It was demonstrated by Bewick, Kunimatsu, and Pons[9] that the modulated UV–visible specular reflectance technique[10-15] could be successfully adapted to infrared studies. Modulation of the electrode potential and synchronous demodulation of the absorbance by phase-sensitive detection, along with signal-averaging techniques, lead to detection sensitivity good enough to observe submonolayer quantities of adsorbates. The feasibility of such studies without the use of an infrared laser source has been questioned.[16]

These first infrared reflectance spectroelectrochemical experiments were made with a dispersive instrument; this technique is known as electrochemically modulated infrared spectroscopy[17] (EMIRS); the extension to Fourier transform instrumentation is generally known as subtractively normalized interfacial FTIR spectroscopy[18] (SNIFTIRS). Another interfacial infrared method, polarization modulated infrared reflection absorption spectroscopy (IRRAS), is also widely used. Polarization modulation has been used to obtain spectra of species on electrode surfaces[19,20] with both dispersive[21] and Fourier transform instruments.[22,23] Difference spectra are obtained with EMIRS and SNIFTIRS: the spectrum measured is that due to the difference in vibrational structure of species at the interface at two electrode potentials. IRRAS spectra are typically obtained at a single potential.

These methods have proven to be useful for studies involving (a) the identification and reactions of adsorbed and nonadsorbed electrochemical reaction intermediates, both neutral and ionic; (b) the surface bonding, intermolecular interaction, and dynamics of adsorbates and the effects on these properties of electric fields; and (c) monitoring the potential-dependent concentrations of molecular and ionic species, both adsorbed and in the electric double layer. Studies of this kind have been made at many types of electrodes, including well-defined single crystals, chemically modified surfaces, semiconductor electrodes, and a number of polycrystalline metal electrodes.

In the following sections theoretical bases for the techniques are outlined, and the results of a variety of experiments are reviewed (q.v.[24]).

II. Experimental Details

Spectrometers capable of measuring absorbances on the order of 10^{-2}–10^{-6} are required for the detection of adsorbed and double- or diffusion-layer species. Two major problems affect the sensitivity of the measurements. The first is the large absorption of most of the radiation by the bulk solvent; this is especially serious if the solvent is water, which absorbs strongly throughout most of the mid- and far-infrared regions. Additionally, absorbance due to trace amounts of water, which may be present in nonaqueous solvents, usually interferes with absorbance of species being studied. The second problem is, of course, that the number of molecules under study is usually very small, oftentimes less than a monolayer (a few tenths of a nanomole). In the following sections some of the experimental methods that are used to overcome the problems of sensitivity and solvent absorption are presented.

A. Cell Design

The problem of solvent absorption is minimized by using a thin-layer cell (Figure 1). An infrared transparent window is mounted at one end of the cell. The working electrode, usually a flat polished metal disk,

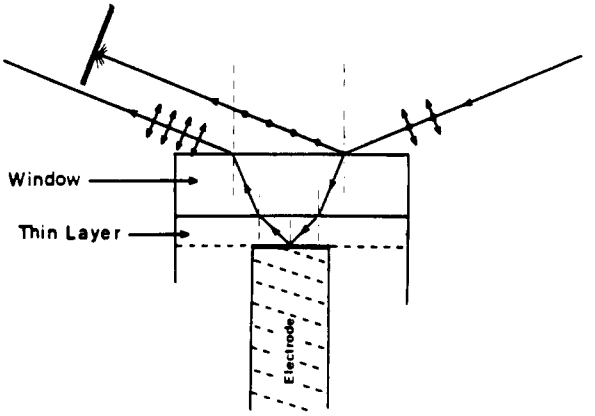

Figure 1. Reflectance arrangement for infrared spectroelectrochemistry employing a thin layer.

is positioned close to the window so that a thin layer of solution (typically on the order of a few microns) is trapped between the window and the electrode. Incident infrared radiation passing through the window and thin layer of solution onto the mirror electrode surface is reflected back out of the thin layer cell and is subsequently focused onto the detector.

The choice of window material depends on the spectral region of interest and on the solvent. Examples of infrared window materials for the mid-infrared region include calcium fluoride, silicon, and zinc selenide, each of which may be used with a variety of aqueous and nonaqueous electrolytes. For the far-infrared region polyethylene is usually employed.

The electrode mounting procedure involves affixing a polished mirror disk of the electrode material at the end of a glass syringe plunger, with the back side of the disk being electrically connected to a wire leading out of the cell (Figure 2). A Luggin reference probe is positioned about 1 mm from the edge of the working electrode. The secondary electrode is typically a platinum wire placed behind the working electrode in a configuration that minimizes solution resistance and provides as symmetric a current distribution pattern to the working electrode as possible.

B. Acquisition of Spectra

The thin-layer cell arrangement still exhibits large solvent and electrolyte absorption. Signal-to-noise enhancement is accomplished through the use of phase-sensitive detection and/or signal-averaging techniques. When a dispersive spectrometer is used, the potential is modulated at a frequency dictated by the type of detector used (1–10 Hz for Golay type detectors up to about 1 kHz for cooled solid-state detectors such as a mercury–cadmium–tellurium type). Phase-sensitive detection is used to synchronously demodulate the measured reflectance at a fixed wavelength. The wavelength is incrementally scanned over the desired spectral region and the signal integrated at each wavelength. Signal averaging of several spectra further enhances the signal-to-noise ratio. With an FTIR instrument, the variation of reflectance with frequency is monitored at constant potential. Usually a few number of interferograms are obtained at two different potentials, and the process is repeated until the desired signal-to-noise ratio is obtained. The two single-beam spectra are differenced and ratioed to the intensity at

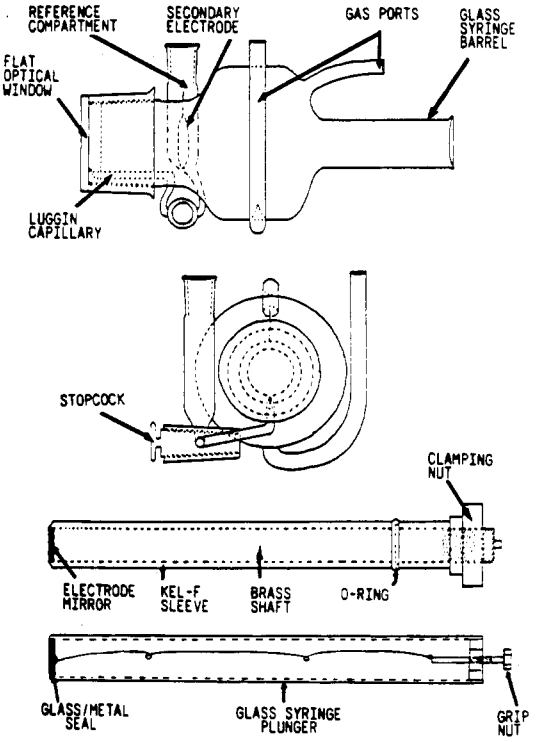

Figure 2. Design of the infrared spectroelectrochemical cell.

one potential to obtain the final normalized spectrum. The result in both cases is a difference spectrum with magnitude $\Delta R/R$

$$\frac{\Delta R(\nu)}{R} = \frac{R_2(\nu) - R_1(\nu)}{R_1(\nu)} \quad (1)$$

R_1 and R_2 are the reflectances at the two electrode potentials. For small values of $\Delta R/R$, this quantity is proportional to absorbance. Both positive and negative bands may be observed. Positive bands are due to absorbances from species present at the base potential E_1, while negative bands are due to absorbers prevalent at the second potential E_2. The measured spectrum shows only changes in reflectance caused by changes in potential. Since the spectra of the bulk solvent, atmosphere, and electrolyte generally do not change with potential, they are effectively nulled when ratioed.

A change in reflectance can result from a change in potential for a number of reasons. These include changes in the coverage of species adsorbed on the electrode, changes in the nature of bonding of adsorbed species, migration of ions into or out of the optical path, and electron-transfer reactions that consume and/or generate species in solution or on the electrode surface. A change in band intensity or the appearance of new bands may result. A band position may change due to changes in the frequency of the oscillator as the strength of bonding to the surface is changed with electrode potential. In addition, the reflectivity of the electrode material itself may change as a result of a potential step; this is a manifestation of the electroreflectance effect. However, in the infrared region, this effect may usually be ignored since its contribution is small and usually linear in wavelength across the entire infrared region. Kunimatsu[27] has described how to obtain single-sided EMIRS spectra by potential sweep techniques.

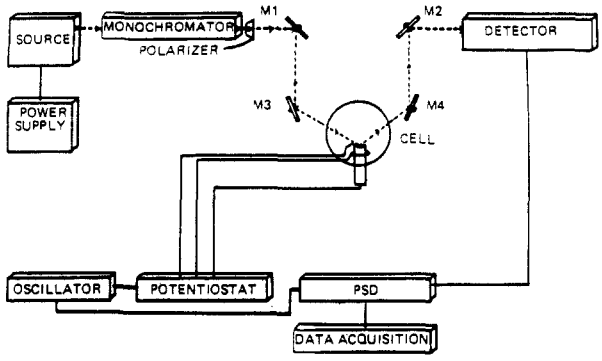

Figure 3. EMIRS instrumentation.

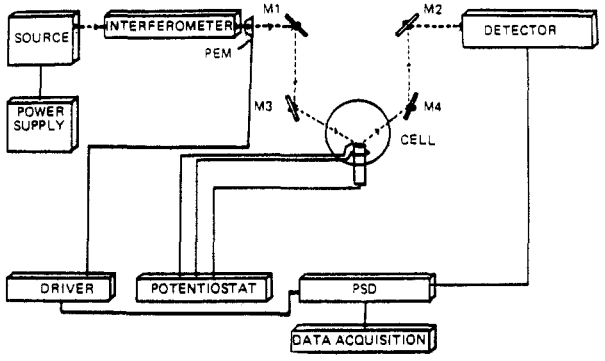

Figure 4. IRRAS instrumentation.

C. EMIRS

Experimental Details of the EMIRS technique have been published.[27] The EMIRS experimental apparatus is shown in Figure 3. A high-throughput dispersive monochromator must be employed, and special optics are employed to accommodate the spectroelectrochemical cell. A Nernst filament operated at an abnormally high temperature serves as the infrared source. Although this reduces the source lifetime, the increased intensity increases throughput significantly. A variety of detectors have been used, including both solid-state types and modified Golay detectors. A polarizer is placed in the incident beam in order in order to eliminate s-polarized radiation. The cell compartment and spectrometer are purged with dry nitrogen to eliminate atmospheric carbon dioxide and water. A commercial instrument is available.

D. IRRAS

In this technique, the infrared radiation is modulated between parallel and perpendicularly polarized components with a high-frequency photoelastic modulator. The principle of the operation of this device has been described.[28] The technique is sensitive to species close to the surface (vide infra). The detected ac signal is then demodulated by a lock-in amplifier, and a spectrum is obtained. This technique has been applied to the study of adsorbed molecules on metals in the gas phase[19,20,29] as well as electrochemical systems.[21] The IRRAS experimental setup is shown in Figure 4. IRRAS is used with both dispersive spectrometers and Fourier transform instruments.[30] In Fourier transform infrared reflection absorption spectroscopy[31] (FT-IRRAS) the detector signal is divided into two channels for signal normalization. One signal is processed normally, and the interferogram, which is equivalent to the

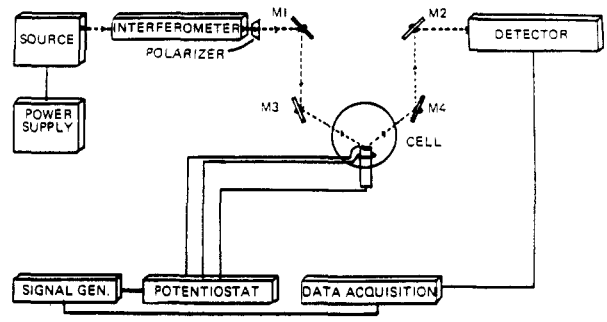

Figure 5. SNIFTIRS instrumentation.

integrated beam intensity in time ($I_p + I_s$), is stored. The other signal is demodulated at the photoelastic modulator frequency, giving an interferogram proportional to ($I_p - I_s$), which is in turn stored in the instrument computer. These stored interferograms are then Fourier transformed and ratioed to give a normalized intensity $(I_p - I_s)/(I_p + I_s)$, which is proportional to absorbance. Sum and difference interferograms are alternately sampled during the same interferometer mirror scan. The normalized ratio calculation allows for cancellation of the source wavelength dependence, detector response, and absorption of solution species some distance from the electrode surface, since I_p and I_s are attenuated equally throughout the beam path (except near the electrode surface). Interferences due to the solvent do exist, however, since s-polarized light is insensitive to species some distance from the electrode surface.[32] Solvent absorbance may be removed from the spectra by subtraction techniques. If a dispersive infrared instrument is used for IRRAS, the quantity ($I_p + I_s$) is obtained by chopping the incident beam at a frequency f_c. The difference signal ($I_p - I_s$) is obtained by using the photoelastic modulator (operated at a frequency f_m) in conjunction with a fixed polarizer. The photoelastic modulator causes phase retardation between $+\pi$ and $-\pi$ radians at f_m. Since a retardation at $+\pi$ radians is the same as that at $-\pi$ radians, the difference in intensities is modulated at double the frequency of the photoelastic modulator, or $2f_m$. The modulation scheme then produces different signal intensities at $2f_m$ and $2f_m + f_c$, and demodulation at $2f_m$ results in the desired spectrum.

E. SNIFTIRS

The instrumentation for this FTIR technique is shown in Figure 5. The multiplex advantage of the Fourier transform technique allows for very rapid spectral acquisition times, but there is lower noise discrimination per scan than in EMIRS. The time to obtain spectra by each technique at the same sensitivity is therefore approximately the same.

The sensitivity of the SNIFTIRS technique depends on many factors. The use of high-intensity sources and attention to careful optical design are important considerations. Sensitivity can be increased by using high-resolution A/D converters that increase dynamic range. However, detectors are usually nonlinear in their response with respect to high-intensity optical flux, so care must be taken when this approach is used. The natural form of the interferogram places extreme demands on the instrument electronics. The intensity of the center burst is high, but it contains relatively little

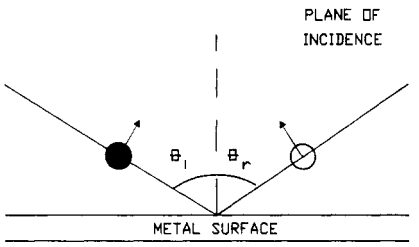

Figure 6. Relative phase components of infrared radiation reflected from a metal surface. p-Polarized radiation is shifted about 90° upon reflection from the surface. s-Polarized radiation is shifted approximately 180° for the incident (solid circle) and reflected (open circle) electric field vectors.

spectral information; most of the desired spectral data lie in the wings. The high amplitude of the center burst may limit the dynamic range of the A/D converter, so autoscaling A/D converters that automatically reduce the gain in the region of the center burst may be employed, allowing a greater dynamic range in the wings of the interferogram. Such gain-ranging techniques can be supplemented by optical subtraction methods[36] that null the center burst, plus all other signals that are unrelated to the change in potential. Optical filters that limit the energy range of radiation striking the detector may also be used to decrease the amplitude of the center burst, thereby increasing detector sensitivity and decreasing spectral acquisition times.

Data accumulation may be accomplished by various means. The simple potential step method described above is the most common. This method has several advantages. One is that electronic and mechanical drift over long periods of time are canceled effectively. Secondly, interferences from atmospheric absorbances due to water and carbon dioxide may be easily eliminated by cancellation in the ratioing of the spectra. Next, since substantial product accumulation may occur in some electrochemical systems over long time periods, the measured difference signal could be decreased if the potential is held at a fixed value for a long period of time. Finally, free radicals and other reactive intermediates that attack some infrared window materials are not allowed to accumulate.

While SNIFTIRS has proven to be useful for obtaining vibrational spectra of interfacial species in the mid-infrared region, it is the most convenient technique for obtaining spectral information in the far-infrared region. FTIR spectrometers that enable switching between beam splitters, optical filters, sources, chambers, apertures, and detectors, all while the instrument remains under vacuum, are very useful for measurements in the far-infrared region.

III. Interaction of Infrared Radiation with Adsorbates

A. Surface Selection Rules

The special properties of reflection of electromagnetic radiation from metal surfaces in the infrared region make it possible to obtain information about the orientation of molecular species at the interface. When infrared light is reflected from a metal surface (Figure 6), s-polarized radiation (radiation whose electric field vector component is polarized perpendicular to the plane of incidence) undergoes a phase shift of nearly 180° at all angles of incidence. The incident and reflected waves cancel at the surface, giving rise to a standing wave that has a node near the surface.[25] p-Polarized infrared radiation, or radiation whose electric field vector component is polarized parallel to the incidence plane, undergoes a phase shift that is a function of the angle of incidence. A phase shift of about 90° is attained at a glancing angle of incidence, and a standing wave that has measurable amplitude near the surface results from the interaction of incident and reflected light. Amplitude and angle of incidence relationships for interfaces with known optical parameters may be obtained by solving Fresnel's equations.[25]

Since p-polarized light is the only component of infrared radiation with appreciable field strength at the electrode surface, it alone carries information on vibrations of interfacial species. Greenler[26] was the first to propose that p-polarized infrared radiation carries virtually all of the vibrational absorption information of species adsorbed at a metallic reflecting surface. He further showed that since the electric field intensity increases sharply with angle of incidence up to near grazing (for p-polarized radiation), the absorbance by an oscillator could be expected to increase as well. He showed that the absorption of radiation by an oscillator varies as the square of the cosine of the angle between the electric field vector of the radiation and the oscillating dipole. Hence, optimal absorption is obtained when the component of the dipole derivative with respect to the normal coordinate of an absorbing species is in the same direction as the incident p-polarized radiation. If the infrared beam is incident at very glancing angles, a sizable component of the electric field will lie in a direction perpendicular to the electrode surface. Oscillators with their dipole derivative component more parallel to the surface will have a smaller probability of infrared absorption. In this way the relative intensities of infrared absorption bands can give information regarding molecular orientations on the electrode surface. This distinction between absorbances due to oscillators oriented parallel and perpendicular with respect to the surface is known as the surface selection rule.

In practice, s-polarized radiation, which has virtually no field strength at metal surfaces, is usually filtered, since it contains no useful information for adsorbed species. Distinction between adsorbed and dissolved species may be facilitated by modulation of the polarization and measuring a difference spectrum between reflectances at both s- and p-polarizations. Randomly oriented solution species, which can absorb both s- and p-polarized light equally well, can be distinguished from adsorbed species, which can absorb only p-polarized radiation. If the difference spectrum is computed by subtracting reflectances measured with each polarization, the resulting difference spectrum will be due to only adsorbed species. Polarization modulation at a fixed electrode potential is an important technique in that it differentiates between adsorbed and dissolved species. However, modulation of electrode potential changes the field strength of the solution near the electrode surface. This change can affect the vibrational frequency of dissolved species through several mechanisms (including ion pairing). This can lead to an erroneous assignment of a solution band to that of an adsorbed species (changes in vibrational frequency with

potential are usually considered to arise only from surface-adsorbed species).

B. Electrochemical Stark Effect and Vibronic Coupling

Spectra of adsorbed species on electrodes are often characterized by changes in their vibrational frequencies with potential. Two mechanisms have been proposed in an effort to explain this shift in band position with potential. One explanation involves molecular orbital considerations, while the other is based on the effect of the strong electric field across the double layer on polarizable electrons of an adsorbed molecule. In the chemical mechanism, electrons can be donated from filled adsorbate orbitals of proper symmetry to empty metal orbitals through σ overlap. The metal can then back-donate electrons from filled d orbitals to empty π^* adsorbate antibonding orbitals. The vibrational frequency of an adsorbed molecule may either increase or decrease with respect to an unadsorbed (solution) species depending upon the relative contributions of σ- and π-bonding interactions. The frequency of absorption of an adsorbed moiety (with respect to solution species) will decrease if the π-bonding interaction dominates, while the frequency will decrease if the σ-bonding interaction is more important. When the electrode potential is made more negative, the adsorbate–metal bond is weakened, owing to charge donation from the metal into adsorbate π^* orbitals. Thus the band frequency shifts to lower wavenumber. Conversely, if the charge on the electrode is made more positive, a shift to higher frequency results due to a strengthening of the bond between the metal and adsorbed species.

The electric field mechanism (sometimes called the electrochemical Stark effect) involves coupling of highly polarizable electrons of the adsorbate with the strong electric field across the electrochemical double layer. The Gouy–Chapman–Stern model[37] predicts that, if the electrolyte concentration is high (on the order of 1 M), most of the potential drop will be approximately linear with distance and will occur within a few angstroms of the electrode surface. An adsorbed species can act as a dielectric across which the largest portion of the potential drop will occur. Very high electric fields (on the order of 10^9 V m^{-1}) are predicted exist in the double layer. Interaction of this electric field with the dipole moment of an adsorbed molecule can lead to changes in the molecular vibrational frequency.

Intensities of certain adsorbate infrared-active modes may be enhanced by altering the electric field across the electrochemical double layer. Such electric field effects may be significant for adsorbed species in which large changes in the polarizability with bond distance ($d\alpha/dr$) exist. The intensity of a vibrational transition is given by

$$B = \frac{2\pi^2\nu T}{\epsilon_0 hc}\mathbf{P}_{fi}^2 \qquad (2)$$

where ν is the frequency of the infrared transition, h is Planck's constant, c is the velocity of light, T is the number of absorbing dipoles per cross-sectional area in the light path, ϵ_0 is the permittivity of free space, and $\mathbf{P}_{fi}$ is the transition dipole matrix element. The dipole moment operator may be expressed as

$$\mathbf{P} = \mathbf{P}_0 + \mathbf{P}_{ind} \qquad (3)$$

where

$$\mathbf{P}_{ind} = E_z\alpha_{zz} \qquad (4)$$

Here, E_z is the magnitude of the electric field normal to the surface and α_{zz} is the polarizability of the adsorbate molecule in a direction normal to the electrode surface. Taylor series expansion of the dipole moment and the polarizability to second order gives the final expression for the transition dipole moment:[38]

$$\mathbf{P}_{fi} = \left\langle \psi_f\left(\frac{d\mu}{dr}\right)r\psi_i \right\rangle + E\left\langle \psi_f\left(\frac{d\alpha}{dr}\right)r\psi_i \right\rangle \qquad (5)$$

An adsorbed species that has a component of the dipole moment derivative normal to the electrode surface will give rise to a normally infrared-active vibrational band. If a sizable component of the polarizability derivative lies in this direction, the absorption band may be enhanced if the electric field is increased in magnitude. Furthermore, large values of the electric field can induce a vibrational mode for an adsorbed species with large values of the polarizability derivative.[39] In this manner molecules that are adsorbed flat on the electrode surface can give rise to weak vibrational absorption spectra and thereby apparently violate the surface selection rule.[38]

Both molecular orbital arguments and electric field considerations may be used to explain observed potential-dependent shifts of absorption frequency of adsorbed species, and complementary methods such as SERS can be used to establish which mechanism is the more important for a concerned system. Indeed, both contributions may be important in some systems and, furthermore, orientational changes may be induced by changes in electrode potential.

IV. Applications

A variety of systems have been studied by electrochemical infrared spectroscopy. In the following sections, we discuss applications to electrocatalytic reactions, molecular adsorption, double-layer studies, the detection and identification of ion radicals, ion adsorption, and the formation of solid phases on electrode surfaces. Additionally, theoretical methods that are used to analyze spectra of adsorbed species and quantitatively account for their potential-dependent frequency shifts are described.

A. Studies of Electrocatalysis

In electrocatalytic reactions intermediates are frequently chemisorbed species. Reaction rates and mechanisms can vary from one electrode material to another, for adsorbed intermediates at some surfaces may in some instances poison the electrode surface and impede electrocatalysis. For example, anodic oxidation of small organic fuels such as methanol and formaldehyde leads to adsorbed intermediate species that lower reaction efficiency at platinum electrodes. In addition reactants and/or products may be chemisorbed and the reaction rate affected. The nature of adsorbate bonding to the surface, and interactions of adsorbates with other adsorbed species and solution species, may be conveniently studied by infrared spectroelectrochemical techniques.

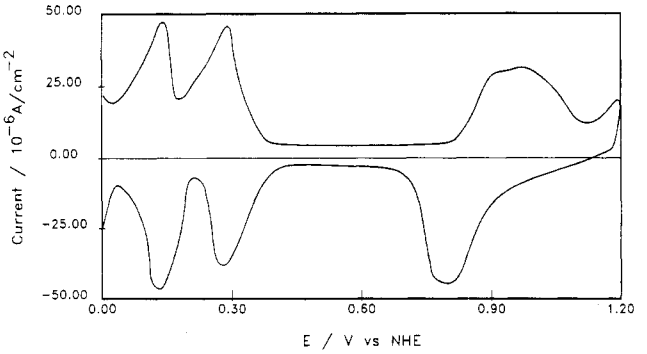

Figure 7. Cyclic voltammetry of 0.10 M H_2SO_4 at a platinum electrode.

1. Adsorption of Hydrogen

A catalytic reaction of technological importance is the evolution of hydrogen by cathodic proton reduction from aqueous acid to give hydrogen. The mechanism for hydrogen evolution involves adsorption of hydrogen atoms. Figure 7 shows a typical cyclic voltammogram of a solution of sulfuric acid at a platinum electrode. The current at negative potentials is due first to proton reduction, giving adsorbed hydrogen, of which there are two types: weakly and strongly adsorbed. The weakly adsorbed species, which is believed to bond to platinum atoms above the metal surface and to hydrogen bond to surrounding water molecules, gives rise to the current peak observed at less positive potentials. The second peak at more positive potentials is due to the oxidation of hydrogen that is strongly adsorbed. The adsorption of this species is believed to result in hydrogen atoms that are buried just inside the platinum metal surface. The peaks observed at very positive potentials are due to platinum oxide formation.

Hydrogen adsorption on Pt[40] and Rh[41] electrodes in acid solutions has been studied by EMIRS. Potential modulation between two limits in the double-layer region (the region between the oxidation of strongly adsorbed hydrogen and platinum oxidation) gives rise to a small base-line shift, which was attributed to the electroreflectance effect. When the potential is modulated between a potential in the double-layer region and a potential negative that of the region where hydrogen is strongly adsorbed, the base-line shifts become larger, but no absorption bands appear in the spectrum. The view that strongly adsorbed hydrogen is buried within the metal and does not interact with surrounding water molecules is consistent with these results; no bands due to water reorganization were observed. Potential modulation between a potential within the double-layer region and a potential negative that of weakly adsorbed hydrogen gives rise to absorption bands that correspond to the vibrational modes of water. An increase in the amount of water present in the double layer is suggested by the sign of the absorption bands. Spectra obtained in solutions of H_2O, D_2O, and HDO gave evidence that weakly adsorbed hydrogen atoms exist in a layer immediately above to the platinum surface. Evidence showed that these hydrogen atom species were likely bonded both to surface platinum atoms and to water dimers (through hydrogen bonds) in the adjacent solution.

Recent work[41] on polycrystalline Pt, Rh, Ir, and single-crystal Pt(111) electrodes in acid solution has identified a new type of adsorbed hydrogen. An adsorption band at 2090 cm^{-1} has been assigned to a hydrogen atom coordinated on top of the surface metal atom. The authors conclude that this new species is the intermediate in the hydrogen evolution reaction from correlations between the potential dependence of the band intensity and the rate of hydrogen formation.

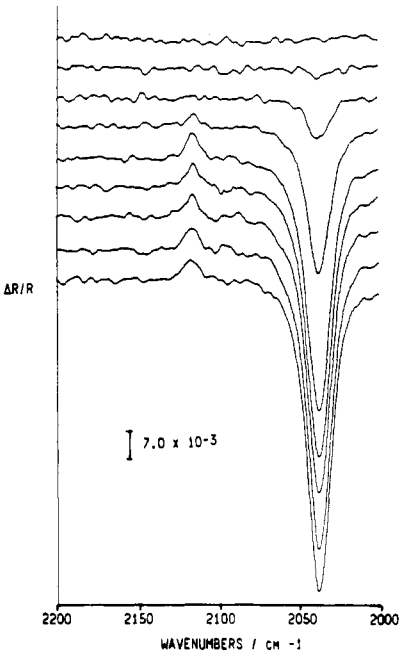

Figure 8. SNIFTIRS spectra of $Fe(CN)_6^{4-}$ oxidation at a Pt electrode using the staircase potential modulation method. The lowest trace was taken at 0.0 V, the next lowest trace was taken at +0.10 V, and the subsequent traces were recorded at 0.05-V increments up to +0.60 V (vs SCE). Base potential = +0.80 V.

2. Oxidation of Organic Molecules That Form Adsorbed CO[42-70]

While this class of reactions represents important catalytic processes, we will discuss it in the section on adsorbed neutral intermediates (section B.1).

3. The Ferrocyanide/Ferricyanide System

In aqueous systems, the ferrocyanide/ferricyanide redox couple has been considered as a model system for the study of heterogeneous electron-transfer reactions. The oxidation/reduction reaction is thought to occur through an outer-sphere electron-transfer mechanism. It has recently been shown, however, that the reaction is much more complex and involves adsorbed species. The electron-transfer rate is also dependent on the electrolyte composition,[71,72] and there is adsorption of complex ions at the electrode surface.[73,74] SERS[75] and SNIFTIRS[76] have been employed in efforts to examine the role of the electrode surface in this electron-transfer process. Figure 8 shows the difference spectra due to the oxidation of ferrocyanide as a function of potential. Instead of the usual square wave potential modulation program, a staircase potential program was used. One hundred interferograms were collected at each potential and were then ratioed to data taken at −0.20 V (the base potential). This technique prevents the loss of information (through signal averaging) regarding species that are irreversibly adsorbed to the electrode surface. The band that appears at 2040 cm^{-1} was assigned to a C≡N stretching mode of $Fe(CN)_6^{4-}$, and the band direction

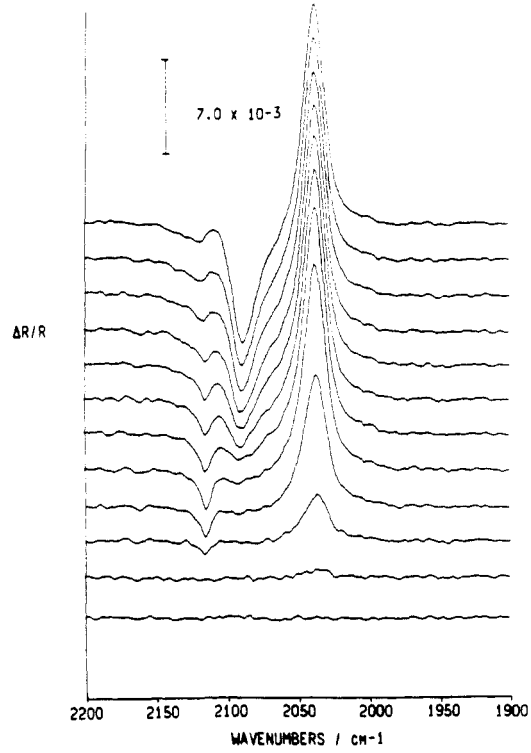

Figure 9. Same as Figure 8 using $Fe(CN)_6^{3-}$. Potentials vary from +0.30 V (top) to −0.20 V (bottom).

indicates that this species is being depleted at higher potentials. Adsorbed $Fe(CN)_6^{3-}$ gives rise to the band at 2114 cm^{-1}; the intensity of this band increases with potential and reaches a maximum at a potential slightly lower than the potential where the band due to $Fe(CN)_6^{4-}$ reaches a maximum. Formation of the surface species, followed by decomposition at higher potentials, is suggested. Additional structure at 2092 and 2061 cm^{-1} is observed; the lower wavenumber band has been assigned to solution CN^- presumably formed from $Fe(CN)_6^{3-}$ decomposition at high potentials.

The same experiment was performed with ferricyanide as the substrate. Figure 9 shows the SNIFTIRS spectra of $Fe(CN)_6^{3-}$ reduction using the staircase potential program method. No evidence existed for the production of a new adsorbed species following $Fe(CN)_6^{3-}$ reduction. Furthermore, bands at 2092 and 2061 cm^{-1} are absent, suggesting no desorption of adsorbed species. The results indicated that the intermediate species is adsorbed irreversibly at high positive potentials. If the adsorption were not irreversible, bands corresponding to the disappearance of adsorbed species would appear. The conclusion was that $Fe(CN)_6^{3-}$ is adsorbed irreversibly at the electrode surface, and at high positive potentials this species decomposes to form a new adsorbate and solution cyanide ion. SERS experiments have suggested that both ferricyanide and ferrocyanide are adsorbed during the electrochemical reaction.[75]

4. SO_2 Oxidation

The oxidation of sulfur dioxide on metal electrodes is of interest for its application in a variety of industrial processes. Electrochemical oxidation of SO_2 results in the formation of adsorbed poisons on the electrode surface. An in situ infrared spectroscopic study of SO_2 oxidation on Pt was undertaken in an effort to fully characterize the surface species partaking in the catalytic process.[38b,77] SNIFTIRS spectra of this oxidation at platinum confirmed electrochemical studies that suggested that separate mechanisms operate when the oxidation occurs on clean and oxide-covered platinum surfaces. A major product of the oxidation is adsorbed dithionate. Additionally, reduction of this adsorbed product formed SO_2 and water, a process not previously observed. The pertinent reactions were postulated to be

$$2SO_2 + 6H_2O \rightleftarrows S_2O_6^{2-} + 4H_3O^+ + 2e^-$$

when the reaction occurs on clean platinum at potentials and

$$SO_2(ads) + PtO + 3H_2O \rightleftarrows SO_4^{2-}(ads) + 2H_3O^+ + Pt$$

when the reaction occurs in the presence of platinum oxide. It was also concluded that sulfite intermediate was not present in the mechanism.

B. Adsorption of Neutral Species

1. Adsorbed CO

Electrocatalytic reactions involving small organic molecules such as methanol, formic acid, and formaldehyde are of interest in fuel cells.[42] Oxidation of these species gives rise to strongly adsorbed intermediates that poison the electrode surface by blocking reactive sites. CO_2 reduction yields similar intermediates. These reactions have been studied extensively by conventional electrochemical methods.[43-46] Coulometric and radiometric experiments indicate that the poison is either COH(ads)[45] or CO(ads).[47-50] EMIRS has been used to study the oxidation of methanol on Pt,[51-53] formic acid on Pt, Rh, and Pd,[54-58] and ethylene glycol on Pt.[59,60] A series of strongly adsorbed carbon monoxide species have been found to be present during the oxidation of these molecules on all three metals. Three distinct adsorbed CO species have been assigned to the observed bands. A band at 2100 cm^{-1} is attributed to a perpendicularly adsorbed molecule associated with a single metal atom ("linear" adsorbed CO: $-C\equiv O$). A C–O stretch near 1900 cm^{-1} has been attributed to CO adsorbed in a bridged site between two metal atoms ("bridge-bonded" CO: $>C{=}O$), and a band in the 1850-cm^{-1} region has been assigned to a CO(ads) species that interacts with three surface atoms ($>C{-}O$). Band assignments were made from gas-phase studies.[61] In these studies, the C–O stretching frequency of each CO(ads) species increases with surface coverage. Similar coverage-dependent spectra were obtained in the in situ electrochemical experiments; spectral dependence on the electrode potential and on the nature of the metal was also observed. The number and relative amounts of each CO(ads) species depend on factors such as surface coverage and electrode history. Identification of specific CO(ads) species on metal surfaces has been confirmed by in situ infrared spectroelectrochemical studies on the direct adsorption of CO from solution. EMIRS[61] and IRRAS[21,22,63,64] have been employed to examine CO adsorption from CO dissolved in aqueous acid solutions. The results from these studies, which gave information regarding the behavior of specific adsorbed CO species, have been used to

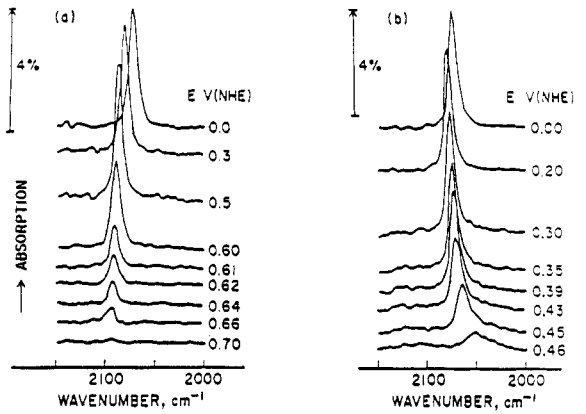

Figure 10. FT-IRRAS spectra of CO adsorbed on Pt: (a) potential = +0.40 V vs NHE; (b) potential = +0.05 V vs NHE. Solution is 0.5 M H_2SO_4/H_2O; the reference potential was +0.80 V.

identify the adsorbates present during the oxidation of the organic molecules.

FT-IRRAS spectra of adsorbed CO (Figure 10) were obtained from CO dissolved in 0.5 M sulfuric acid solution.[64] Figure 10a shows the behavior of adsorbed CO at potentials in the double-layer region, while Figure 10b shows the behavior of CO(ads) at potentials where adsorbed hydrogen is present. In the double-layer region, CO(ads) band intensity is constant at potentials above +0.6 V, but intensity decreases markedly at higher potentials due to oxidation of adsorbed CO to CO_2. When CO_2 is formed, the band due to linearly adsorbed CO disappears. The bandwidth due to linear CO(ads) is constant, and the band shifts with potential in a linear manner (30 cm^{-1} V^{-1}). This linear potential shift is observed regardless of coverage, and this sort of potential dependence has been ascribed to oxidation at islands of adsorbed CO. Since the shift is linear with potential change, the implication is that most of the CO(ads) experiences a constant environment as the potential changes. For systems where CO is coadsorbed with hydrogen, oxidation occurs at less positive potentials. The linear CO(ads) band intensity is constant up to potentials where CO_2 oxidation occurs and then sharply decreases. The increase in frequency with potential is linear up to about +0.2 V, whereupon the frequency begins to decrease. CO coadsorption with hydrogen has been suggested to occur randomly, rather than along edges of "islands". The early oxidation that occurs at approximately +0.4 V has been attributed to oxidation of a species formed by the reaction of CO(ads) with H(ads). Additionally, the observed increase in line width and decrease in band frequency are indicative of a decrease in dipole–dipole coupling between adjacent CO(ads) species. This view is consistent with the contention that there is a random distribution of adsorbed CO throughout the adsorbed hydrogen layer.

There have been several studies concerning the oxidation of methanol and formic acid. Kunimatsu[55] showed that an intermediate CO(ads) moiety is the predominant surface species in methanol and formic acid oxidation. A linearly bonded adsorbed CO species is certainly present, but other surface species were also observed. Hahn et al.[58] examined the oxidation of formic acid on Rh and observed a bridge-bonded CO(ads) and an adsorbed formate species, in addition to linear CO(ads). Sun and co-workers[57] proposed a mechanism for formic acid oxidation on Pt(100) and Pt(111) surfaces, based on an EMIRS study. This work supplemented voltammetric studies[45] wherein the presence of linear CO(ads) was found to be a function of the Pt crystal orientation. Multiple internal reflectance Fourier transform (MIRFTIR) methods have recently been employed to examine intermediates in methanol oxidation on Pt in basic solution.[65] A primary intermediate (CO(ads)) was found to poison the electrode surface. The poison was found to be absent during the oxidation of methanol to formate on Fe, and methanol oxidation occurred at a lower potential than on Pt. EMIRS studies on Pt adsorbates in the oxidation of methanol in acid medium[52,53] show evidence for at least three types of CO adsorbates. These include both linear and bridge-bonded CO(ads), along with a third species that is purported to have a carbonyl C=O bond. Polarization-modulated IRRAS has also been employed to study the potential dependence of CO(ads) species resulting from CH_3OH and HCOOH oxidation.[66] In that work it was found that CO(ads) poisons the surface well below 0.5 V, while above this potential CH_3OH and HCOOH can be electrooxidized much more quickly than at lower potentials. This decrease in catalytic activity below about 0.5 V was found to be due mainly to poisoning by linear CO(ads).

Adsorbed intermediates from the oxidation of ethylene glycol have been studied by EMIRS in both acidic and basic media.[60] It was found that linear CO(ads) predominated in strongly acidic solution, but both linear and bridge-bonded CO(ads) were present in highly alkaline media. It was suggested that other adsorbed species may also be present.

Carbon dioxide reduction has been studied by the EMIRS technique.[67] Bands due to both linear and bridge-bonded CO(ads) intermediates were detected, and it was concluded that CO_2 reduction to adsorbed CO takes place by reaction with adsorbed hydrogen. Also, the bridged intermediate species was found to form more readily by reduction from CO_2 than by direct adsorption of carbon monoxide or formic acid under conditions that exclude CO_2 formation.

The oxidation of formaldehyde on Pt in the presence and absence of lead was studied by EMIRS.[68] It was determined that deposition of submonolayer amounts of lead onto the platinum electrode surface partially blocked the formation of adsorbed poisons. The coverage of linear CO(ads) was found to be reduced in the presence of lead, as evidenced by a decrease in band intensity and a shift in the CO band frequency. Bridge-bonded CO(ads) species were not observed when lead was deposited. Formaldehyde oxidation on Pt, Ir, and Rh in base has been examined by EMIRS,[69] and the mechanism of oxidation has been proposed to be similar on all three metals. An intermediate *gem*-diol anion to give formate and adsorbed hydrogen was suggested based partly on previous electrochemical work.[70]

At constant coverage, the integrated band intensity of adsorbed CO is potential independent.[63] The band positions of adsorbed CO are independent of coverage (in the absence of coadsorbates) but depend on the potential. Intensities of vibrational bands of highly polarizable molecules, as previously noted, may vary with potential, in addition to shifting in frequency. Ray

and Anderson[78] have modeled CO adsorption on Pt using a technique that combines one-electron orbital energies with atom–atom repulsion energies. Increases in C–O vibrational frequencies with increases in potential are predicted, together with a corresponding decrease in the metal–carbon frequency. The results were explained in terms of decreased mixing of Pt d orbitals with π^* orbitals on CO(ads) as the potential was increased, thereby strengthening the C–O bond and weakening the Pt–C bond. Although donation of σ electrons to the metal by CO increases with increased electrode potential, this interaction is too weak to counter the reduced π overlap. Similar models have been applied to the case of cyanide adsorbed on silver.[79]

The effect of the electric field on the occupancy of the $2\pi^*$ orbital of CO(ads) on Pt has been discussed.[80] It was suggested that the electric field shifts the energy of the antibonding state, thereby affecting its occupancy. The antibonding orbital occupancy was calculated as a function of the electrical potential, resulting in a shift in the CO stretching frequency of 30 cm^{-1}/V. Lambert[81] has proposed a Stark-type mechanism wherein the frequency shifts due to the interaction of the electric field with polarizable electrons of the adsorbed molecule. An expression for the Stark tuning rate (the change in vibrational frequency with electric field) was derived based on the total Hamiltonian for an adsorbed molecule. The total energy of the system is changed due to interaction of the dipole moment with the external electric field, which is a function of the Hamiltonian. A Stark tuning rate for CO adsorbed on Ni(110) of 30 cm^{-1}/V was predicted. Korzeniewski et al.[82] derived a potential energy function describing the interactions of CO(ads) on Pt(111), and a linear shift of CO(ads) vibrational frequency as a function of binding energy was computed. Additionally, the calculated Stark tuning rate was in agreement with the value predicted by Lambert.[81] This work provided theoretical evidence that the observed linear frequency shift with potential is due to a combination of chemical bonding and electric field interactions.

Carbon monoxide adsorption on platinum surfaces has been studied by infrared spectroscopy in the gas phase on Pt(111) surfaces.[83,84] Two bands appear in the spectrum under ultrahigh-vacuum conditions: one at low coverage at about 2065 cm^{-1}, and another at 1850 cm^{-1} at intermediate and high coverages; the assignments were discussed above. The spectra of adsorbed CO species have also been taken in aqueous media on polycrystalline platinum surfaces.[21,22,62,63] Under these in situ conditions a band is observed at 2060 cm^{-1}, and the band position shifts to higher wavenumber as the electrode potential is made more positive. A linear shift of 30 cm^{-1}/V (in agreement with theoretically predicted and gas-phase Stark values[81,82]) is observed for saturation coverage of CO(ads). FT-IRRAS spectra of CO(ads) on polycrystalline Pt are shown in Figure 10. The spectra are recorded as a function of applied potential; the base potential was +0.80 V vs SCE, where CO is oxidized to CO_2 and is no longer adsorbed. The observed frequency shift with potential has been proposed to be due to CO adsorbed in islands on the pt surface.[63] CO_2 oxidation is believed to occur at the island edges. The frequency of absorption due to adsorbed molecules was attributed to coupling of adjacent CO(ads) species. This coverage-dependent shift is similar to that observed for CO adsorbed onto Pt from vacuum.[85]

Severson et al.[86] studied the infrared spectra of CO(ads) on Pt at partial coverages in pure ^{12}CO and in mixtures of ^{12}CO and ^{13}CO. A vibrational coupling model was used to interpret the results. The effective coupling in the adlayer was shown to be about twice as large as that observed for CO(ads) on Pt(111) under high-vacuum conditions. Furthermore, the coupling was apparently unchanged with changes in potential. Contributions of adsorbed hydrogen atoms were suggested to cause changes in the infrared spectra of partial coverage CO adlayers, with the implication being that a change in the adlayer structure occurs.

Coverage and potential dependencies of CO adsorbates on Pt in perchloric acid media were studied by using both UV and infrared probes in situ.[87] Two different adsorbed CO species were indicated, and the distribution of these two types of adsorbates was dependent on both potential and coverage. At low coverage, CO(ads) was predominantly in the form of the bridge-bonded species, while at high coverage, linear-bonded CO(ads) was prevalent. CO adsorption on platinum has been studied by FT-IRRAS[88] in the region where hydrogen is adsorbed. It was found that the bridge-bonded species oxidized prior to the linearly adsorbed moiety and that CO oxidation occurred randomly throughout the adlayer. The potential dependence of linear CO(ads) was examined and the results were interpreted in terms of an electrochemical Stark effect.[81,89]

Carbon monoxide adsorption has been studied in alkali solutions.[90] It was found that CO adsorption was enhanced in alkaline media in comparison with adsorption in acidic solutions. This enhanced adsorption was assisted by hydroxide ions, but the nature of the alkali metal ion had little effect. The potential dependence of the C–O stretching frequency was also linear. CO(ads) vibrational spectra have been recorded on platinum electrodes in neutral electrolytes.[91] Several differences in the CO(ads) spectra compared with the spectra in acidic electrolytes were noted, including increased predominance of bridge-bonded adsorbed CO species at very low coverages. EMIRS spectra of CO adsorbed on gold electrodes have been obtained in both acidic and basic media,[92] with comparisons in CO adsorbates in both media being made. Also, CO(ads) electrooxidation in both acid and base was examined.

IRRAS spectra of CO adsorbed on Pd and Pt have been obtained in the presence of other adsorbates besides H(ads).[93] Frequency shifts in the band position of bridged CO(ads) on Pd were explained in terms of changes in dipole–dipole coupling between bridged CO adsorbates along with shifts in the potential of zero charge. On Pt, the band frequency and intensity of linear CO(ads) changed with changes in concentration of coadsorbates; however, on Pd, no such shifts were observed for the linear CO(ads) species. Other workers have examined the effects of coadsorbates on adsorbed CO, in attempts to study dipole–dipole coupling phenomena.

2. *Adsorption of Difluorobenzene*

Aromatic molecules, which can adsorb parallel to the electrode surface, may interact with the metal surface

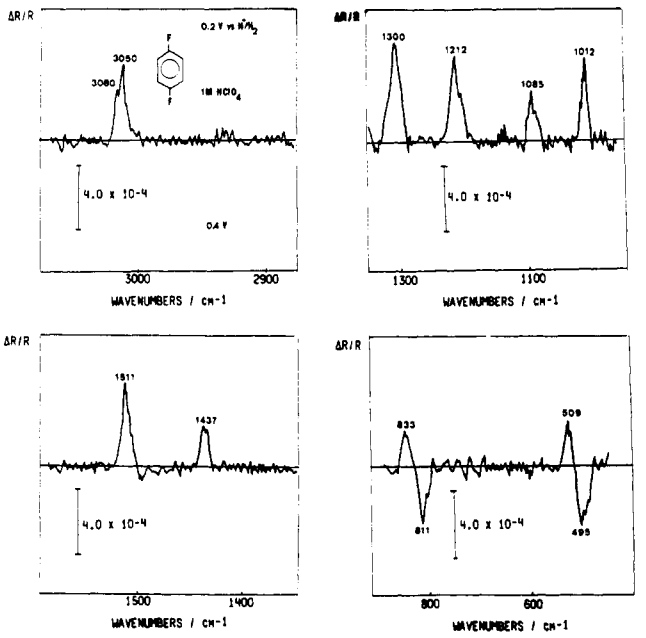

Figure 11. SNIFTIRS spectrum of *p*-difluorobenzene at a platinum electrode. The modulation potential was +0.20 to +0.40 V vs NHE. The solution was 5 mM in *p*-difluorobenzene in 1.0 M perchloric acid.

through π orbitals. This type of bonding interaction would most likely involve σ donation of electrons in π orbitals of the adsorbed species into empty metal orbitals, with d→p π back-bonding from metal d orbitals into empty adsorbate π^* orbitals. Such an interaction would weaken certain bonds in the adsorbed molecule and shift their vibrational modes to lower wavenumber. Imposition of a more positive potential would tend to strengthen the σ donation and weaken the d→π^* back-bonding.

The adsorption of difluorobenzene on Pt electrodes was studied by SNIFTIRS.[94] At low concentrations (less than monolayer coverage) this molecule is predicted to be adsorbed flat on the electrode surface.[95] The SNIFTIRS spectrum of *p*-difluorobenzene is shown in Figure 11. Positive $\Delta R/R$ bands are due to solution-soluble *p*-difluorobenzene present at the base potential (+0.20 V vs NHE). Negative bands are due to adsorbed species at +0.40 V. The only observable adsorbate bands occur at 495 and 811 cm^{-1}, and these were assigned to out-of-plane B_{3u} ring modes; these bands are slightly shifted in frequency with respect to solution bands. Bands due to in-plane modes are not observed: this is evidence that the molecule is flatly adsorbed at this concentration.

The behavior of the B_{3u} mode as the potential is stepped from the base potential to increasingly positive potentials is shown in Figure 12. The band position of the adsorbed species shifts to lower wavenumber as the potential is increased. Charge transfer from the adsorbate to the metal can occur through overlap of π orbitals of the adsorbate with metal orbitals of similar symmetry. The bond order in the adsorbed molecule is decreased by this interaction, so the vibrational frequency shifts to lower wavenumber. The solution species band is unaffected by changes in potential.

As the concentration of adsorbate is deliberately increased, the band intensities due to B_{3u} vibrational modes of both adsorbate and solution species increase.

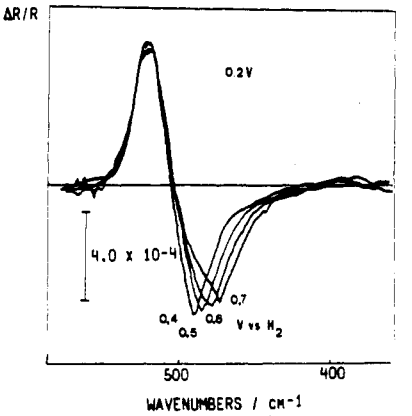

Figure 12. SNIFTIRS spectra of *p*-difluorobenzene in the region of the B_{3u} ring bending mode as a function of the modulation potential. Other parameters are the same as in Figure 11.

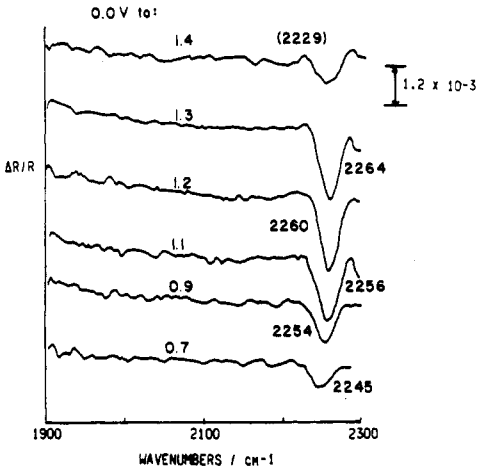

Figure 13. EMIRS spectra of benzonitrile adsorbed on Au as a function of potential. The solution was 20 mM in benzonitrile in 0.10 M sulfuric acid. The potential modulation limits are shown in the figure; the modulation frequency was 8.5 Hz. Base potential was 0.0 V vs NHE.

This can be taken as evidence that the concentration of adsorbate increases with increased solution *p*-difluorobenzene concentration. Also, at high *p*-difluorobenzene concentrations, new bands appear due to in-plane ring modes of adsorbed species. These bands are due to skewed packing of the molecule on the surface; the results agreed with those of Hubbard et al.[95] In that work, configurations were determined by thin-layer electrochemical techniques as a function of concentration and temperature.

3. *Adsorbed Benzonitrile*

EMIRS was used to study benzonitrile adsorption on gold electrodes;[96] the effect of potential on the difference spectra in the C≡N stretching region is shown in Figure 13. The negative $\Delta R/R$ band at 2229–2264 cm^{-1} shifts toward higher wavenumber and increases in intensity as the stepped potential is made more positive, except at very positive potentials, where the formation of gold oxide inhibits benzonitrile adsorption. This band has been attributed to the C≡N stretching mode of benzonitrile adsorbed perpendicular to the metal surface, with bonding to the surface presumably occurring through the nitrogen atom. Increased adsorption at higher potentials is suggested by the increase in band intensity as the potential is increased. It was

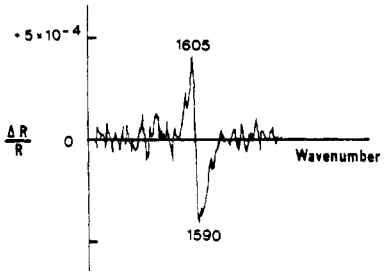

Figure 14. SNIFTIRS spectrum in the ring stretching region for anthracene reduction on Pt. The potential was modulated from −1.50 to −2.50 V vs Ag/Ag^+.

argued that the nitrogen atom can σ donate electrons to the metal through the lone-pair orbital. Since the lone-pair orbital is slightly antibonding, electron donation to the metal from that orbital can strengthen the C≡N bond. In turn, back-donation of electron density from the metal to π^* adsorbate orbitals may occur.

Additional evidence for the perpendicular orientation of benzonitrile on gold was determined from EMIRS spectra taken in the region where in-plane benzonitrile ring modes were expected to occur. Bands appeared at 1480 and 1595 cm^{-1}, corresponding to A_1 ring modes. If the molecule were adsorbed parallel to the surface, these modes would not be observable unless a Stark-type mechanism was applicable. If this were indeed the case, the band intensity due to the C≡N stretching vibration would be expected to be much smaller due to the low polarizability of the bond. Similar behavior of the benzonitrile C–N stretch has been observed in SNIFTIRS[97] and SERS[98] experiments, giving further evidence that the adsorption interaction is through the CN group.

4. Adsorption of Anthracene and Pyrene

Symmetric vibrational modes have been activated for molecules with a center of inversion.[38,99] The SNIFTIRS spectrum of adsorbed anthracene on platinum is shown in Figure 14. The positive band has been assigned to the A_g symmetric stretch of neutral anthracene, while the negative band has been attributed to the A_g mode of the anion radical. The proposed mechanism by which this mode is activated is through coupling of the electric field in the double layer with the polarizable electrons in the anthracene molecule.[38]

Further evidence of the interaction of the strong electric field in the double layer with polarizable electrons of adsorbed molecules was obtained from studies on adsorbed pyrene on Pt.[38,99,100] SNIFTIRS spectra of pyrene at low concentration in acetonitrile are shown in Figure 15 as a function of potential. It has been shown that similar molecules at this concentration are adsorbed parallel to the electrode surface.[101] The potential modulation limits were set between values where no electrochemical reaction occurred; thus bands appearing in the difference spectra are due to the changing electric field across the double layer. Raman spectra of pyrene dissolved in solution were obtained, and bands due to the totally symmetric (A_g) stretching mode[102] were observed at nearly identical wavenumber as the band appearing in the difference spectra. Hence this potential-dependent SNIFTIRS band has been attributed to the A_g vibrational mode of pyrene induced by the electric field.

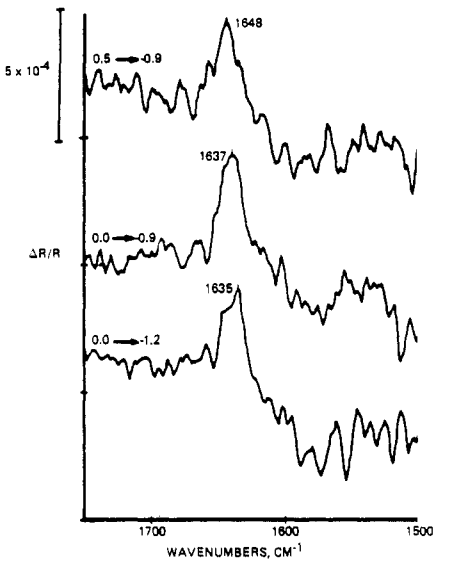

Figure 15. Difference spectra of pyrene on platinum obtained via the SNIFTIRS technique. Solution is 0.5 mM pyrene in CH_3CN/0.10 M tetra-*n*-butylammonium tetrafluoroborate (TBAF) supporting electrolyte. Potentials are vs the Ag/Ag^+ reference.

5. Other Molecular Adsorbates

EMIRS studies on adsorbed acrylonitrile[100] have provided further evidence for field-induced absorption by an adsorbed molecular species. Factors such as nonlinear frequency shifts with changes in potential and band intensities that were smaller than would be expected for perpendicularly adsorbed acrylonitrile contributed to this conclusion. Investigations of this kind, involving apparent violations of the surface selection rule, are valuable for surface studies, for the molecular adsorbate orientation may be established unequivocally in many cases.

Solomun[103] examined NO adsorption on palladium electrodes and obtained evidence for a "bent" adsorbed nitrosyl species. A linear NO(ads) moiety was also observed, but the bent adsorbate was observed for the first time. Kumimatsu and Bewick[104] obtained EMIRS spectra of adsorbed water on gold in perchloric acid solution. There is evidence for H_2O(ads) with different degrees of hydrogen bonding: adsorbed water monomers, dimers, and polymers were suggested based on bands occurring at different frequencies and having a variance of bandwidths. The potential dependence of these bands was interpreted in terms of the density of each H_2O(ads) species.

Beden et al. have investigated ethanol adsorption at platinum electrodes by EMIRS.[105] Various potential-dependent bands were observed, with that for linear CO(ads) predominant. There was also evidence for the existence of other adsorbed species, including weakly adsorbed ethanol, adsorbed ethoxy $(CH_3CH_2O)^-$, and an adsorbed ethylate $(CH_3CO)^-$.

C. Adsorption of Ions

1. Adsorbed Cyanide

FT-IRRAS and EMIRS have been used to obtain infrared spectra of cyanide adsorbed on silver and gold surfaces.[23,64,97,106,107] This system has also been studied extensively by SERS methods.[108–113] Combined studies involving SERS with FT-IRRAS[113] and SNIFTIRS[97]

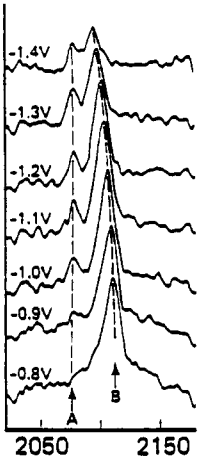

Figure 16. FT-IRRAS spectra of CN^- adsorbed on Ag. Solution contained 0.1 N KCN in 0.1 N K_2SO_4. Reference potential was −1.5 V vs Ag/Ag^+.

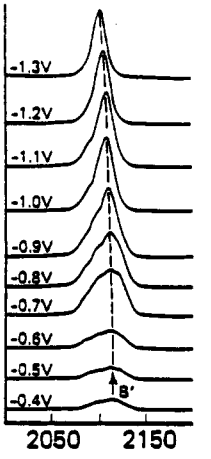

Figure 17. SERS spectra of CN^-(ads) on Ag in the same solution as that described in Figure 16. Surface roughening was accomplished by a redox cycle from −1.0 to +0.5 V and back at a sweep rate of 50 mV/s.

have also been reported. SERS studies on pseudohalide ions have been published.[115,116]

Difference spectra of CN^- on silver obtained by FT-IRRAS methods are shown in Figure 16. The base potential was chosen where no CN^- occurs; positive bands are attributed to species present at the more positive potential. The band appearing at 2080 cm^{-1} has been assigned to solution cyanide, while the band appearing around 2100 cm^{-1} is assigned to linear CN^-(ads); the interaction with the metal surface is through the carbon atom. The intensity of the solution cyanide band (which is present whether s- or p-polarized light is used) reaches a maximum at −1.2 V and decreases thereafter as the potential is made more positive. The intensity of the band attributed to adsorbed cyanide (which is observed only if p-polarized radiation is used) increases as the potential is made more positive, indicating that adsorption is increased at higher positive potentials. It is also observed that the CN^-(ads) band position shifts to higher wavenumber by 30 cm^{-1}/V as the potential is made more positive. The indication is that the mechanism of this potential-dependent shift is similar to that of adsorbed CO.

SERS spectra of this same system are shown in Figure 17. A band is observed at approximately 2100 cm^{-1}; the intensity of this band increases as the potential is made more positive, and the band position shifts with potential by about 28 cm^{-1}/V. The bandwidth of the SERS band exceeds that of the FT-IRRAS band at 2100 cm^{-1} at all potentials and, at more negative potentials, the intensity of the SERS band decreases more rapidly than the band obtained in the infrared experiments. At more positive potentials the SERS bandwidth increases significantly and the band shape becomes more complex. It was concluded that the environment of the SERS-active species may be different from the environment of the infrared-active adsorbed species, where there was no surface roughening. However, similarities in the spectra obtained by both methods indicate that environmental differences are not strong enough to perturb the C≡N stretching frequency nor the band potential dependence. The FT-IRRAS spectra of CN^-(ads) on gold were similar to those obtained on silver.

Polarization modulation infrared spectroscopy of adsorbed cyanide on silver was performed by using a new technique[117] employing the Kretschmann ATR prism configuration.[118] In this way it was possible to effectively reduce absorption due to solution species. The spectra due to CN^-(ads) obtained in this manner compared favorably with SERS results for adsorbed cyanide ion.[79,119] Other studies have appeared where an ATR configuration was employed.[120,121]

2. *Thiocyanate Adsorption*

Thiocyanate adsorption on electrode surfaces has been studied by SERS[97,119,122,123] and by SNIFTIRS.[96,97,123-125] SERS spectra of this system consist of several bands: there is a predominant band at about 2120 cm^{-1}, with less intense bands at 240, 295, 455, and 700 cm^{-1}. The band at 2120 cm^{-1} shifts to higher wavenumber with increase in positive potential by about 12 cm^{-1}/V; this band has been attributed to the C≡N stretching mode of SCN^- adsorbed through the sulfur atom. The bands at 240, 455, and 700 cm^{-1} are assigned to Au–S stretching, N–C–S bending, and C–S stretching modes, respectively. The band at 295 cm^{-1}, attributed to an Au–N stretching mode, appears at more negative potentials, where the 240-cm^{-1} band is reduced in intensity. This has been suggested to be due to reorganization of the surface species, but there is no evidence of this transition in the C≡N stretching region of the spectrum.

SNIFTIRS spectra were compared with SERS results; the spectra taken by both techniques were quite similar. The SNIFTIRS spectra gave rise to a bipolar band in the C≡N stretching region; this was reported to be due to thiocyanate adsorbed through the sulfur atom. A shift in the band to higher wavenumber as the potential is made more negative gives rise to the bipolar nature of the band. As the potential is made more positive, the negative band broadens and shifts to higher wavenumber by 12 cm^{-1}/V. Also, a large positive $\Delta R/R$ band appears at 2065 cm^{-1}, due presumably to the C≡N stretch mode of solution thiocyanate. This band is due to the disappearance of solution species at the higher potentials to form SCN^-(ads).

3. *Other Ionic Adsorbates*

Other ionic species studied by infrared spectroelectrochemical techniques include bisulfate,[126] azide,[97,125]

and cyanate.[97,125] Recent investigations have indicated that the adsorbate spectra are dependent on the nature of the electrolyte species present in the solution, in addition to being potential dependent.

D. Double-Layer Studies

1. Electrolyte Studies

SNIFTIRS has been employed to study changes in the electrical double layer in acetonitrile solutions of various types and concentrations of supporting electrolytes.[128] SNIFTIRS spectra of tetra-*n*-butylammonium tetrafluoroborate (TBAF) in acetonitrile were obtained as a function of applied potential, and strong bands were observed in the 1100-, 1400-, 2350-, and 3000-cm^{-1} regions. The band near 1100 cm^{-1} was assigned to the tetrafluoroborate anion. The intensity of this band was found to change with potential, and this was reported to be due to changes in the relative concentration of the anion as the potential was changed. An increase in potential in a positive direction resulted in an increase in the absorbance due to anion species, since as the potential is made more positive, a larger number of anions are needed to balance the charge on the electrode. The band observed at 2350 cm^{-1} was attributed to adsorbed acetonitrile, since the C≡N stretching frequency of the band was blue shifted with respect to the frequency of this band due to solution species. The intensity of this adsorbed solvent band increased as the potential was made more positive; this was rationalized in terms of increased adsorption of the solvent molecule due to increased electrostatic forces at the higher positive potentials.

Experiments were performed on the same solutions with added water. Bands were observed due to water molecules that were extensively hydrogen bonded. The intensities of these bands were found to be potential dependent and were thus attributed to water molecules associated with the electrolyte anions. Other bands due to water molecules not strongly perturbed by hydrogen bonding were observed. These bands were shown to arise from the formation of a water–acetonitrile complex.[129] Spectra obtained in solutions containing lithium perchlorate as the supporting electrolyte instead of TBAF indicated that the behavior of the $LiClO_4$ electrolyte system is similar to that of the TBAF system.

Studies on electrochemical solvent/electrolyte breakdown processes in TBAF/acetonitrile solutions have been done by using infrared spectroelectrochemistry.[130] It was found that electrolyte anodic breakdown gave the adduct CH_3CNBF_3 as the major product, while cathodic breakdown gave the 3-aminocrotononitrile anion as the major product in very dry solutions. The formation of this product was a consequence of hydrogen dissolved in the metal electrode. If water is present, cathodic breakdown occurs at much less negative potentials than in the absence of water, and acetamide is formed in addition.

Infrared spectroelectrochemistry has been used to examine the influence of ion migration on composition changes in the double layer.[131] The results indicated that potential-dependent cation migration can contribute to charge redistribution, but anion migration predominates when specific anion adsorption is encountered. Some general consequences of ion migration on potential-dependent infrared spectra of adsorbed species were noted.

E. Solution Species

1. Radical Ions and Dianions

There has been a great deal of interest in the electrochemistry of organic radical cations and anions.[42,132] Electrochemical techniques are useful for the study of these species since organic radical ions can be conveniently formed in the electrochemical cell. The first spectroelectrochemical experiments for the study of organic radical ions were performed by UV–visible techniques.[133] Recently, infrared techniques have been applied to the study of the behavior of these species in the diffusion layer. Difference infrared spectra are taken by modulating the potential between a base value where only reactants are present and a value where the product ions are formed. Use of a thin layer enables bulk electrolysis of reactant species on the experimental time scale, thereby enhancing the sensitivity of the technique, for spectra collected at the stepped potential are now due mainly to products.

(a) The Tetracyanoethylene System. The kinetics and the behavior of the tetracyanoethylene (TCNE) system under reductive conditions have been studied in aprotic solvents in the presence of various electrolytes.[96,134-136] The radical anion is formed reversibly, but the rate of dianion formation is dependent on the nature of the supporting electrolyte. Cyclic voltammetry of TCNE in acetonitrile exhibits a reversible wave near 0 V vs Ag/Ag^+, regardless of the nature of the supporting electrolyte. At more negative potentials the dianion is formed. In solutions that contain tetra-*n*-butylammonium tetrafluoroborate (TBAF) as supporting electrolyte, the cyclic voltammetry of the anion/dianion couple shows quasi-reversible behavior at about −0.9 V. In solutions containing lithium perchlorate electrolyte, the potential at which this redox couple occurs is less negative (approximately −0.7 V) and the wave is more reversible. Several factors are responsible for this behavior. These include complexation of the radical anion, a comproportionation reaction involving the dianion and neutral species, and electrode poisoning due to product adsorption. SNIFTIRS has been used to study this system.[96,136]

SNIFTIRS spectra for the formation of $TCNE^-$ and $TCNE^{2-}$ are shown in Figure 18. The thin-layer thickness was approximately 50 μm. The bands were observed regardless of the polarization of the infrared radiation, indicating that the bands are due to dissolved species. In the anion spectra (Figure 18A) bands appear at 2187 and 2146 cm^{-1}; the position and intensity of the bands are independent of the nature of the electrolyte. Conversely, bands due to the dianion (Figure 18B) are strongly dependent on the nature of the supporting electrolyte. Bands appear at 2141 and 2075 cm^{-1} when TBAF is the electrolyte, and these bands shift to 2175 and 2101 cm^{-1} when $LiClO_4$ is the electrolyte. Transmission spectra of TCNE and $TCNE^-$ in acetonitrile have been published.[137] Bands appearing in the transmission spectra of neutral species at 2265 and 2225 cm^{-1} have been assigned to the B_{1u} and B_{2u} C≡N stretching modes, respectively. Transmission spectra

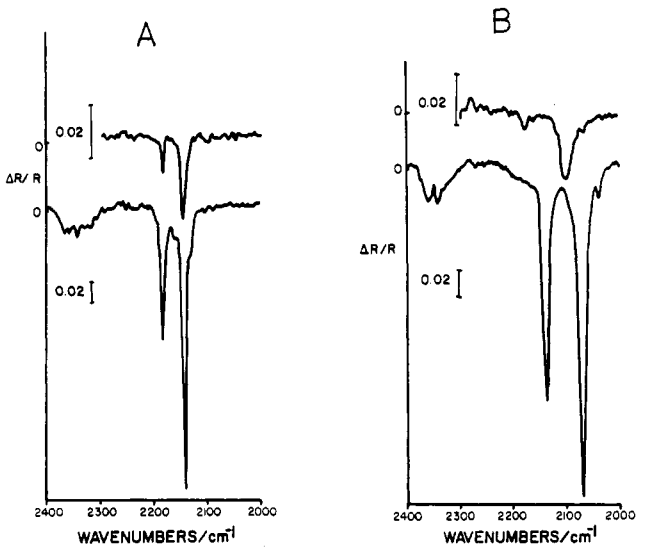

Figure 18. SNIFTIRS spectra for the reduction of TCNE on platinum. Solutions were 5 mM in TCNE in CH_3CN/0.10 M $LiClO_4$ (top spectra) or 0.10 M TBAF (bottom spectra). (A) Formation of the radical anion; pulse modulation +0.5 to −0.5 V vs Ag/Ag^+. (B) Formation of the dianion; pulse modulation +0.5 to −1.2 V (top spectrum) and +0.5 to −2.0 V (bottom spectrum). Thin-layer thickness approximately 50 μm.

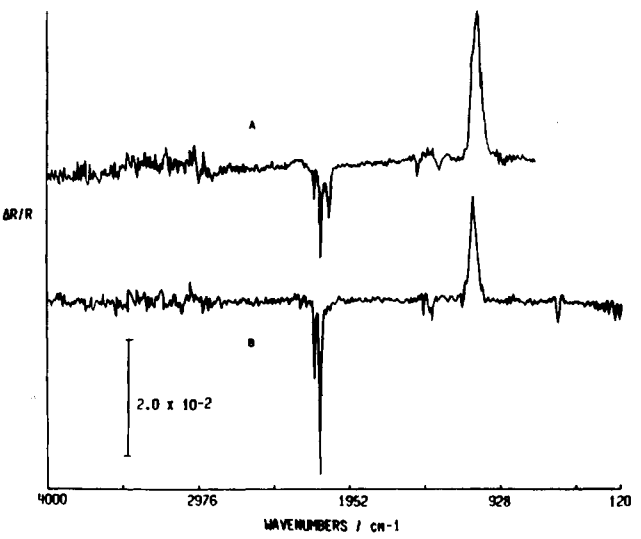

Figure 19. SNIFTIRS spectra obtained during the reduction of TCNE to $TCNE^-$ in acetonitrile. Supporting electrolyte was (A) 0.10 M $LiClO_4$ and (B) 0.10 M TBAF. The potential was modulated between +0.5 and −0.5 V vs Ag/Ag^+; thin-layer thickness approximately 1 μm.

of radical anion generated by electrolysis give rise to bands at 2225, 2185, and 2145 cm^{-1}; the 2225-cm^{-1} band is due to residual neutral species present in the optical path.

The higher wavenumber $TCNE^-$ band has been assigned to the B_{1u} C≡N stretch and the lower wavenumber band has been attributed to the B_{2u} mode.[96] The significant red shifts of these bands were explained as follows. The lowest unoccupied orbital of the neutral species is antibonding, with nodes between the C=C and C≡N bonds. The C≡N bond is weakened when the anion is formed, thereby shifting the C≡N modes to lower energy. For analogous reasons, further bond weakening results when the dianion is formed; hence, even more pronounced red shifting of C≡N stretching bands occurs. However, the dianion bands are not as strongly red shifted when $LiClO_4$ is present in comparison with the case when TBAF is in solution. Strong ion pairing of $TCNE^{2-}$ with Li^+ and weak ion pairing with Bu_4N^+ have been suggested to account for the observed spectral differences. The Li^+ cation, which is small and more polarizing, would tend to remove electron density from the dianion, making the orbital state less antibonding. This interaction would tend to increase the energy of the C≡N bonds, compared to the case where ion-pairing interactions are weak (i.e., when tetrabutylammonium cation is present) and $TCNE^{2-}$ is less stabilized.

A study was conducted in a thin-layer cell (about 1 μm) containing approximately 1 nmol of TCNE. SNIFTIRS spectra for the formation of $TCNE^-$ on Pt are shown in Figure 19. Intense positive $\Delta R/R$ bands are observed at about 1100 cm^{-1} in both electrolytes; these bands are attributed to the loss of the supporting electrolyte anion (ClO_4^- or BF_4^-) as the electrode is charged. In the spectrum obtained in $LiClO_4$ solutions, bands appear at 1420 and 523 cm^{-1}; these have been assigned to the $\nu_2(A_g)$ C=C and $\nu_2(A_g)$ C≡C stretching modes, respectively. The 2187-cm^{-1} solution band has also been attributed to the $\nu_1(A_g)$ C≡N stretching vibration;[76] bands at similar wavenumber have been observed in resonance Raman spectra of $TCNE^-$ in this solvent.[139] The infrared activity of these bands has been attributed to a vibronic interaction wherein the π-electron density, which is highly polarizable, is coupled to the motion of neighboring atoms. This may occur either by strong ion pairing of the electrolyte cation with the radical anion or by dimerization of the monoanions. The symmetric vibrational modes are then activated by distortion of the polarizable anion π-electron cloud to produce a dipole; interactions of this nature have been observed for TCNE complexed with alkali metal cations in the solid state.[137] Frequencies of the C≡N and C=C A_g bands have been observed to shift to lower energies as the electron affinity of the countercation is reduced.[140] However, no shift in the 2187-cm^{-1} band occurred in the difference spectra of $TCNE^-$ when the complexing cation was changed from Li^+ to Bu_4N^+; this would rule out strong ion-pairing interactions between supporting electrolyte cation and $TCNE^-$. There is evidence that the anion radical species exists as a dimer in the solid state but is prevalent as a monomer in solution.[141] Thus it appears that the 2187-cm^{-1} band is due to a normally infrared-active mode that has been shifted to lower wavenumber as a result of these bonding effects.

A new band appears at approximately 2080 cm^{-1} in the $TCNE^-$ difference spectrum in TBAF taken in a 1-μm thin layer (Figure 19B) compared with the spectrum obtained in a much thicker layer (Figure 18A). This band position is close to that of the dianion C≡N stretching frequency in the absence of ion pairing. Also, bands at 1475 and 1325 cm^{-1} appear in the spectrum obtained from a very thin layer. The three new bands have been assigned to modes of an adsorbed TCNE molecule.[76]

SNIFTIRS spectra were studied as a function of TCNE concentration (Figure 20). As expected, bands due to solution species at 2145 and 2185 cm^{-1} increase in intensity with increases in TCNE concentration, but the band at 2080 cm^{-1} remains constant as the concentration of solution TCNE is increased. This is the

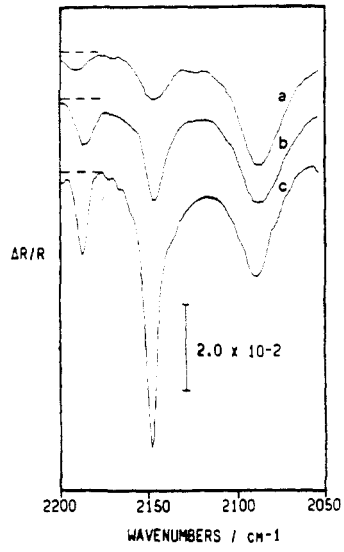

Figure 20. SNIFTIRS spectra for the reduction of TCNE to $TCNE^-$ as a function of the TCNE concentration. Solution concentration of TCNE is (a) 1 mM, (b) 2 mM, and (c) 5 mM. Potential modulation: +0.5 to −0.5 V vs Ag/Ag^+. Solution: 0.1 M $TBAF/CH_3CN$.

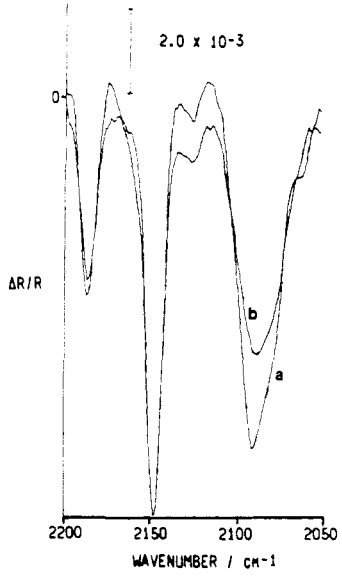

Figure 21. SNIFTIRS spectra for the formation of $TCNE^-$ from TCNE as a function of the polarization of incident light. The spectra were taken with (a) p-polarized radiation and (b) mixed s- and p-polarized light.

expected result for an electrode at maximum equilibrium coverage. Difference spectra taken as a function of the radiation polarization are shown in Figure 21. It is observed that the solution band intensities are unchanged with the light polarization, but the intensity of the 2080-cm^{-1} band is increased if only p-polarized radiation is incident on the electrode surface. It was also noted that the band positions of all spectral bands attributed to surface species were potential dependent. This is strong evidence that the TCNE anion is adsorbed on the electrode surface. Furthermore, the spectra indicate that the $TCNE^-$ adsorbed species are oriented flat on the surface, since bands due to nonequivalent C≡N stretching modes (which would arise from $TCNE^-$ adsorbed edgewise) are absent.

Charge-transfer complex formation at the electrode surface has been attributed to the appearance of bands due to totally symmetric modes.[76] Such interactions have been observed on Ni(111), where donation of electrons from the metal to the adsorbed molecule results in a decrease in bond order and subsequent shifting of the C≡N and C=C stretching modes. Interaction of the polarizable anion with electrons in the metal surface results in activation of these modes. In turn, mode oscillation may cause changes in the molecular dipole moment derivative in a direction normal to the electrode surface. Coupling of the strong electric field to the highly polarizable adsorbate electrons could also induce a dipole in a direction perpendicular to the plane of the surface. It is reasonable to assume that $TCNE^-$ can interact with a Pt surface in a manner similar to its behavior on nickel.

Infrared spectra of tetracyanoquinodimethane (TCNQ) dianions have also been found to be dependent on the nature of the electrolyte.[136] Upon reduction, $TCNQ^-$ was found to behave in a similar manner to $TCNE^-$.

(b) Benzophenone Ketyl Radical. The SNIFTIRS technique has been used to obtain the difference spectrum of the benzophenone ketyl radical[142] in a 1-μm thin layer of solution. The spectrum of the ketyl anion resembled spectra of this species obtained by other means.[143] Bands appeared due to C=O stretching modes of the ketyl anion and neutral benzophenone molecule. ESR data showed that the electron density is highly localized in the carbonyl bond;[144] this results in a large red shift of the C=O stretching mode for the anion state. Other bands appeared in the difference spectrum[142] that were not present in the previously reported transmission spectrum.[143] The appearance of these bands was suggested to be due to interactions between adsorbed ketyl anion and adsorbed solvent molecules.

2. *Inorganic Ions*

(a) Ferrocyanide Complexes. SNIFTIRS has been used to investigate lithium, magnesium, and lanthanum ferrocyanide complexes at platinum and gold interfaces.[145] The data support the existence of complex ions of the type $M_nFe^{II}(CN)_6^{(4-n)-}$, where M pertains to the lithium, magnesium, and lanthanum cations. It was suggested that these complexes retain their octahedral symmetry due to the labilities of the coordinated cations. No evidence was observed for the existence of complex anions of the type $M_nFe^{III}(CN)_6^{(3-n)-}$.

F. Time-Resolved Studies

FTIR spectroscopy has recently been employed to study the kinetics of electrode processes on a millisecond time scale.[146] In time-resolved SNIFTIRS, interferograms are collected as usual, but the electrochemical experiment is delayed sequentially with respect to the interferometer scan. The interferogram is collected as a set of discrete points $I(\delta_i,t_j)$, each corresponding to the intensity of the interference pattern at a specific mirror position and a specific point in time. The electrochemical experiment is triggered at sequentially later times relative to the start of the interferogram. Points of each collected interferogram are then sorted and recombined to yield an interferogram representing a single point in time. A set of interferogram files are stored containing the points $I(\delta_i,t_j)$. These points are sorted and recombined to give inter-

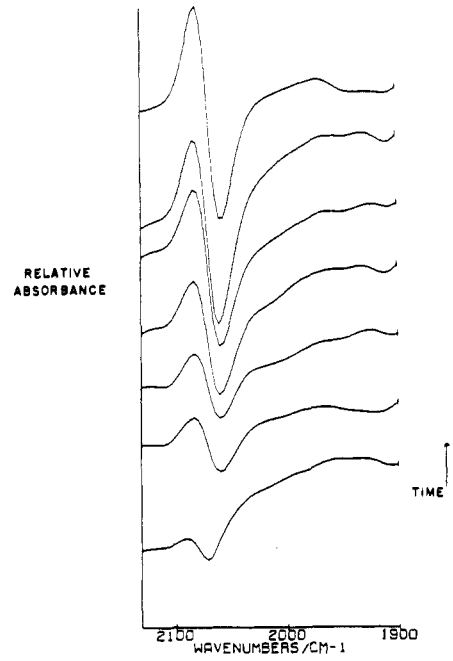

Figure 22. Time-resolved SNIFTIRS spectra of $TCNE^-$(ads) on Pt. The bottom spectrum was obtained 0.001 s after the potential step to −0.8 V; the base potential was +0.6 V vs Ag/Ag^+. Succeeding spectra were taken at 0.001-s intervals.

ferograms that contain the points $I(\delta_i,t_j)$, where $i = j$ for all values of j.[149] Figure 22 shows time-resolved spectra of the TCNE system from a potential modulation between +0.6 and −0.8 V vs Ag/Ag^+. Due to slow charging of the electrode in this particular experiment, TCNE reduction to TCNE dianion takes place only relatively slowly as the migration of ions into the layer develops the charge in the double layer. The upward-pointing band at 2083 cm^{-1} is due to the disappearance of TCNE to form $TCNE^{2-}$, which gives rise to the downward-pointing band at 2065 cm^{-1}. Time-resolved SNIFTIRS studies have also been performed in the far-infrared region at gold electrodes.[147] Studies in the far-infrared region are of interest since in this wavelength region it becomes possible to observe directly the characteristics of metal–adsorbate bonds. In these investigations it was possible to observe the Au–Au fundamental stretch, showing that reflection FTIR spectroscopy may be used to directly observe metal atom vibrations at surfaces. Additionally, lithium nucleation and growth were studied by the time-resolved method, with better than 5-μs resolution. An Au–Li species[147] and an Li–Li vibration[150] were detected.

It has been proposed that transient IRRAS experiments may be possible.[148] Such investigations may be feasible through the use of a tunable infrared laser and a thin-layer cell with well-defined optical properties and a short RC time constant.

G. Surface-Coverage Studies

SNIFTIRS has been used to determine surface coverages of a number of adsorbate species.[151-154] The radiotracer method is used to calibrate infrared peak areas to surface coverage. H_3PO_4 adsorption on platinum and gold electrode surfaces has been studied as a function of concentration and/or potential. On platinum, coverage was found to increase with potential to a maximum value, whereas the coverage decreased with further increases in potential. The coverage was also found to vary in a linear fashion with the logarithm of the H_3PO_4 concentration. A similar study was made for trifluoromethanesulfonic acid adsorption on Pt. Adsorption of $CF_3SO_3^-$ was found to be lower than that of H_3PO_4 and to vary less with potential. Thiourea adsorption on iron electrodes was also studied, and good agreement between surface coverages obtained by infrared and radiotracer methods was obtained over a wide potential range.

H. Nonmetal Surfaces

1. Semiconductor Surfaces

Studies on adsorption on semiconductor surfaces have been carried out on p-CdTe photoelectrodes[155,156] using SNIFTIRS. Spectra reportedly due to adsorbed CO_2^- were obtained under illumination in an aprotic solvent saturated with carbon dioxide.

Other studies have been conducted at silicon/solution interfaces using IRRAS.[157-160] Evidence in the near-infrared region for the slow oxidation of the semiconductor electrode surface was observed.[157] In addition, the presence of nonequivalent adsorbate sites at the interface was indicated. Investigations of the absorption of surface states at the n-Si/electrolyte interface resulted in the observation of two kinds of surface states with distinct optical properties.[158] The results were compared with spectra obtained at the gold/solution interface, which gave a potential-dependent electromodulation absorption in line with the predictions of Harrick.[161] Measured optical cross sections were well accounted for in terms of reorganizationless surface states by using a modified version of the Lucovsky model.[162] However, oxidation-induced surface states gave rise to unexpected potential-dependent behavior which could be explained by taking into account the effects of reorganization (atomic relaxation) during changes of population of the surface states. Silicon surfaces exposed to methanol were characterized by impedance and EMIRS techniques and also in a vacuum by Kelvin probe measurements.[159] The EMIRS data showed the attachment of methoxy and trimethylsiloxy groups on the Si surface. Further efforts have been undertaken in characterizing specific adsorbed species at the silicon/solution interface in the presence of various solvents and electrolytes.[160] Numerous adsorbed species were identified under a variety of conditions, and conclusions regarding the locations of surface states were made.

Raman scattering and FTIR reflectance spectroscopies have been used to examine p-InP/oxide surfaces.[163] Thin films grown in slightly acidic tartaric acid solutions were found to be primarily indium dihydrogen phosphate. This layer was found to significantly reduce band bending, a result similar to that obtained in open-circuit photovoltage measurements. It was demonstrated that the growth of anodic oxide on p-InP introduces surface states that act as surface recombination centers.

2. Carbon Electrodes

A study of adsorption of species on glassy carbon electrodes has been reported.[164] SNIFTIRS spectral evidence for the adsorption of phosphate and sulfate

ions was obtained at potentials of +1.0 V vs SCE, but no evidence was found for the adsorption of perchlorate ions under similar conditions. Infrared studies at carbon electrodes are generally difficult.

I. Films on Electrode Surfaces

IRRAS has been used to study the formation of films on silver surfaces from electrochemical reactions of cyanide,[23,64,114] and SNIFTIRS has been employed to study films due to the electrochemical reaction of cyanide and thiocyanate on platinum and silver electrodes.[96,124] SNIFTIRS spectra obtained in the silver/cyanide system showed bands due to $[Ag(CN)_2]^-$ and $[Ag(CN)_3]^{2-}$ complexes[165] in solution. At more positive potentials $[Ag(CN)_3]^{2-}$ is converted to $[Ag(CN)_2]^-$, and with continued increases in potential $[Ag(CN)_2]^-$ is converted to AgCN, which was found to precipitate onto the electrode surface. SNIFTIRS studies of the silver/thiocyanate system at platinum electrodes indicate that SCN^- is oxidized mainly to thiocyanogen $[(SCN)_2]$ in acetonitrile and to CO_2, SO_4^{2-}, and NO_2^- in aqueous solution. Silver, however, is oxidized at less positive potentials than is platinum, and the oxidation products have been attributed to complexation and/or precipitation of Ag^+ with CN^-. The behavior of this system has been studied extensively in both aqueous and nonaqueous solvents.[96]

Infrared reflection spectroscopy has been applied to the study of adsorbed monolayer films of *n*-alkanoic acids on oxidized aluminum substrates.[166] The results indicated that close-packed assemblies are formed with extended alkyl tails oriented with their chain axes tilted in a direction away from normal to the surface. The spectra further showed that chemisorption occurs by proton dissociation to form carboxylate species. Examinations of line widths and peak positions of the carboxylate stretching modes suggested a variety of surface-binding geometries.

Reflection–adsorption infrared spectroscopy has been applied to the characterization of platinum electrode surfaces in perchloric acid solutions.[121] In 1.0 M $HClO_4$, adsorbed hydronium was found to be present on the surface at negative potentials (vs Ag/AgCl); this adsorbed hydronium species was reported to stabilize water adsorption at the electrode surface. Adsorbed hydronium also reduced CO adsorption and caused an upward shift in the CO stretching frequency. CO(ads) coverage was determined to be maximized in the potential region between 0 and +0.4 V. At potentials greater than 0.5 V it was found that OH was adsorbed on the electrode surface, and this blocked CO adsorption. At more positive potentials (greater than +1.2 V) anodic oxidation occurs, with the resulting formation of a partially hydrated $Pt(OH)_4$ surface layer; the thickness of this surface film increased with further increases in potential. Adsorbed species found to be present in 1.0 M NaOH solutions were found to be similar to those in adsorption of acids. However, anodic oxidation in base gave rise to a different type of surface film than that observed in acidic solution.

A method for measuring linear dichroism of polymer films has been developed by combining FTIR and polarization modulation techniques.[167] The combination of a polarizer and a photoelastic modulator was used to describe the dichroic difference $[\Delta A = A(\parallel) - A(\perp)]$ in a single measurement. This method was shown to provide an order of magnitude improvement in signal to noise over FTIR methods using fixed polarization.

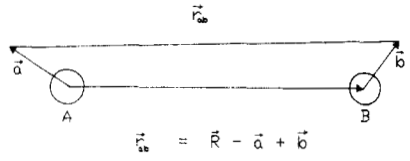

Figure 23. Vectorial displacements $\vec{a}$ and $\vec{b}$ of atoms A and B from their equilibrium positions.

Fourier transform photothermal spectroscopy has been used in conjunction with cyclic voltammetry to characterize graphite electrodes modified by the deposition of iron-containing films.[168] The results indicate the presence of surface-bound Prussian blue, Berlin green, and Everett's salt, depending on the electrode potential and the nature of the supporting electrolyte cation. It has been shown by infrared reflection spectroscopy that Prussian blue is formed at platinum and gold electrodes when ferrocyanide oxidation occurs at high positive potentials.[169]

A new technique based on attenuated total reflectance (ATR) allows depth profiling of films on electrode surfaces.[170] The technique, called angle-resolved infrared spectroelectrochemistry (ARIRS), involves varying the angle of incidence of the infrared beam. This reportedly enables data sampling at various depths from the electrode surface. The technique was used to study the structure of electrochromic nickel oxide films.

V. Theoretical Methods

In this section a semiempirical theoretical method developed to describe the effects of perturbations on the vibrational spectra of adsorbed species is outlined.[82] Other theoretical treatments have been presented based on ab initio calculations for model[89,171,172] adsorbates at metal atom clusters. Conventional methods of normal coordinate analysis are not well suited for the description of systems that are affected by external perturbations. Hence, a method of analysis that considers the effects of external perturbations (for example, an externally applied electrode potential) on vibrational spectra of adsorbed species is desired.

In the present method, Cartesian force constants are obtained for the displacement of atoms from their equilibrium positions, and a potential energy function for the system is developed as the sum of pairwise potentials operating between the bonded and nonbonded atoms in the molecule. Perturbations are introduced as additional pairwise terms. Force constants are derived for the system by Taylor series expansion (to second order) of the individual potential energy functions. The Cartesian force constant matrix is transformed to the normal coordinate force constant matrix, and normal mode vibrational frequencies are obtained directly. A full description of the Taylor expansion and its applications have been outlined.[173–176] In the analysis, one considers a scalar function

$$F(\mathbf{r}) = Y_{00}(\hat{r})[4^{1/2}\pi g(r)] \qquad (6)$$

where $Y_{lm}(\hat{r})$ are spherical harmonic functions. We expand about two centers A and B separated by a vectorial distance **R**; this is illustrated in Figure 23,

where $\mathbf{r} = \mathbf{R} - \mathbf{a} + \mathbf{b}$. The Taylor series expansion about the two centers is

$$F(\mathbf{R} - \mathbf{a} + \mathbf{b}) = \sum_n (1/n!)(\mathbf{a}\cdot\nabla + \mathbf{b}\cdot\nabla)^n F(\mathbf{r}) \quad (7)$$

In this form the series is evaluated most easily in Fourier transform space. Defining the Fourier transform of $F(\mathbf{r})$

$$F(\mathbf{r}) = \frac{1}{(2\pi)^3}\int \mathrm{d}^3k\, f(k)\, \exp[-(i\mathbf{k}\cdot\mathbf{r})] \quad (8)$$

and substituting (8) into (6) with subsequent expansion yields

$$F(\mathbf{R} - \mathbf{a} + \mathbf{b}) = (4\pi)^2 \sum_{n=0}^{\infty}(1/n!)\sum_{s=0}^{n}\binom{n}{s}a^{(n-s)}(-b)^s \sum_{l,m}[(2l_1 + 1)(2l_2 + 1)]^{-1/2}(l_1 l_2 00|10)(l_1 l_2 m_1 m_2|lm)A_{n-s,l_1}A_{s,l_2}Y_{l_1 m_2}(\hat{\mathbf{b}})Y^*_{lm}(\hat{\mathbf{R}})\, I_{nl}(R) \quad (9)$$

where $(L_1L_2M_1M_2|LM)$ is a Clebsch–Gordon coefficient,[177] $\binom{n}{s}$ is the binomial coefficient, and A_{nl} is given by[175a]

$$A_{nl} = \frac{n!(2l+1)}{(n-1)!!(n+l+1)!!} \quad \text{for } n \geq 1 \text{ with } n-1 \text{ even}$$

$$A_{nl} = 0 \quad \text{for } n < 1 \text{ with } n-1 \text{ odd} \quad (10)$$

and $I_{nl}(R)$ is expressed by

$$I_{nl}(R) = \frac{(-1)^{n-l}}{(4\pi)^{1/2}}R^l\left(\frac{1}{R}\frac{\mathrm{d}}{\mathrm{d}R}\right)^l\left(\frac{1}{R}\frac{\mathrm{d}}{\mathrm{d}R}\right)^{n-l}Rg(R) \quad (11)$$

When the binomial and Clebsch–Gordon coefficients are evaluated at first and second order, the expression is simplified. The first-order term can be expressed in a form useful for finding the optimum configuration of the system:

$$g_1(\mathbf{R} - \mathbf{a} + \mathbf{b}) = 4^{1/2}\pi[(a-b)\cdot R]I_{11}(R)/R \quad (12)$$

where $I_{11}(R) = (1/4\pi)^{1/2}\,\mathrm{d}g/\mathrm{d}R$. The second-order term may be written

$$g_2(\mathbf{R} - \mathbf{a} + \mathbf{b}) = (1/2)(\mathbf{a} - \mathbf{b})^{\mathrm{T}}\mathbf{K}(a - b) \quad (13)$$

where $(\mathbf{a} - \mathbf{b})^{\mathrm{T}} = v^{\mathrm{T}}$, and v^{T} is the transpose of the column vector $\mathbf{v}$. Solving for the force constants yields the Cartesian diagonal elements of the matrix $\mathbf{K}$, which are given by

$$k_{ii} = (1/3)(4\pi)^{1/2}[I_{20}(R) + (2X_i^2 - X_j^2)I_{22}(R)/R^2] \quad (14)$$

in which X_i is the ith Cartesian component ($i = x, y, z$) of the vector $\mathbf{R}$ between the centers A and B. The off-diagonal Cartesian elements are

$$k_{ij} = 4^{1/2}\pi X_i X_j I_{22}(R)/R^2 \quad (15)$$

and the radial quantities $I_{20}(R)$ and $I_{22}(R)$ are given by

$$I_{20}(R) = \left\{\frac{2}{R}\frac{\mathrm{d}g}{\mathrm{d}R} + \frac{\mathrm{d}^2g}{\mathrm{d}R^2}\right\}(1/4\pi)^{1/2} \quad (16)$$

and

$$I_{22}(R) = \left\{\frac{\mathrm{d}^2g}{\mathrm{d}R^2} - \frac{1}{R}\frac{\mathrm{d}g}{\mathrm{d}R}\right\}(1/4\pi)^{1/2} \quad (17)$$

For a Morse potential the radial quantities I_{20} and I_{22} are written

$$I_{20}^{\mathrm{M}}(R) = 2a^2D\,\exp\{a(R_0 - R)\}[2\,\exp\{a(R_0 - R)\} \times (1 - \{1/aR\}) - 1 + 2/aR] \quad (18)$$

and

$$I_{22}^{\mathrm{M}}(R) = 2a^2D\,\exp\{a(R_0 - R)\}[\exp\{a(R_0 - R)\} \times (2 + \{1/aR\}) - 1 + 1/aR] \quad (19)$$

In the limit of $R \rightarrow R_0$ these quantities reduce to

$$I_{20}(R) = I_{22}(R) = 2aD^2 \quad (20)$$

For the case of a Lennard-Jones potential, the radial quantities I_{20} and I_{22} are expressed

$$I_{20}^{\mathrm{LJ}}(R) = \frac{12\epsilon}{R^2}(c/R)^6[11(c/R)^6 - 5] \quad (21)$$

and

$$I_{22}^{\mathrm{LJ}}(R) = \frac{24\epsilon}{R^2}(c/R)^6[7(c/R)^6 - 4] \quad (22)$$

In the limit of $R \rightarrow R_0 = c$, we have

$$I_{20}(R) = I_{22}(R) = 72\epsilon/c^2 \quad (23)$$

On inspection of eq 9, observe that there are two kinds of second-order contributions to the force constant matrix. The first arises when $n = 2$, $s = 0, 2$; these are the only allowed values of s in this limit. The index values contribute to the diagonal elements of the force constant matrix. The Cartesian force constants correspond to the oscillation of atom A in a static field. The vector $\mathbf{R}$ connects bodies A and B, but the displacement of atom B does not enter at this point. The complete potential energy function is a sum of pairwise potentials for each interaction, so for species A there is a sum of contributions to the overall force constant from interactions with all surrounding species. The second term arises when $n = s = 2$; these values contribute to the off-diagonal elements of the Cartesian force constant matrix. The Cartesian displacements of body A are coupled bilinearly with the displacements of body B. Only two of these dynamical interactions exist for each pair of atoms, and the summation is divided by $^1/_2$ to prevent double counting of terms.

The use of Cartesian force constants makes it possible to account in a simple manner for environmental effects on the vibrational analysis. The only requirement is an appropriate form of the potential energy function for which the quantities $I_{20}(R)$ and $I_{22}(R)$ may be obtained. The method has been applied to the analysis of the potential-dependent frequency shift of adsorbed CO on a Pt(111) surface.[82] The potential energy of the system is developed as a sum of pairwise interactions for contributions of the various atoms in the system; i.e.

$$V_{\mathrm{tot}} = V_{\mathrm{CO}} + V_{\mathrm{CS}} + V_{\mathrm{OS}} \quad (24)$$

Here, V_{CO} is the Morse potential representing the bonding in a carbon monoxide molecule, which is expressed as

$$V_{\mathrm{CO}} = D\,\exp[a(r^\circ_{\mathrm{CO}} - r_{\mathrm{CO}})]\{\exp[a(r^\circ_{\mathrm{CO}} - r_{\mathrm{CO}})] - 2\} \quad (25)$$

D, a, and r°_{CO} are the values for an isolated CO molecule, and r_{CO} is the carbon–oxygen separation distance. The potential function V_{CS} describes the interaction of

TABLE I. Parameters Used for the Overall Potential Energy Function

potential	parameters
V_{CO}	D = 11.11 eV, a = 2.31 Å^{-1}, $r°_{CO}$ = 1.13 Å
V_{CS}	ϵ = 2.04 eV, c = 1.81 Å
V_{OS}	D' = 0.13 eV, γ = 0.86 Å^{-1}, $r°_{Oi}$ = 4.6 Å

the carbon atom with the metal surface. Using a Lennard-Jones potential to describe the interaction of the carbon with each of the metal atoms of the Pt(111) surface, we have that V_{CS} is the sum of interactions

$$V_{CS} = \epsilon\sum_i (c/r_{Ci})^6[(c/r_{Ci})^6 - 2] \quad (26)$$

The radii r_{Ci} are to the distances between the carbon atom and each interactive platinum atom i. The surface model used[82] consisted of 14 Pt atoms in a (111) arrangement. The term V_{OS} represents the interaction between the oxygen atom and the metal surface. Using a sum of Morse potentials to express the potential due to the interaction of the oxygen with the metal surface atoms, we have

$$V_{OS} = \sum D' \exp[\gamma(r°_{Oi} - r_{Oi})]\{\exp[\gamma(r°_{Oi} - r_{Oi})] - 2\} \quad (27)$$

where r_{Oi} are to the distances between the oxygen atom and each ith platinum atom.

For the interaction potential, the parameters used are listed in Table I. V_{CO} parameters were chosen to be those for CO in the gas phase. In V_{OS}, the parameter $r°_{Oi}$ was chosen as a repulsive term. The remaining parameters in V_{CS} and V_{OS} were optimized by a least-squares fit to the experimental binding energies and the C–O and Pt–C vibrational frequencies obtained under ultrahigh-vacuum conditions for both linear and bridged CO(ads) sites. The Newton–Raphson method was used to optimize C–O and Pt–C bond lengths; the geometry was optimized with the CO molecule bound normal to the metal surface with the carbon atom nearest to the surface. The binding energy was computed from the difference between the total energy (eq 24) and the dissociation energy of an isolated CO molecule. Parameters in V_{CS} and V_{OS} potential contributions were refined until calculated binding energies and vibrational frequencies agreed with experimental values.

It was shown[82] that for linear changes in the binding energies (D' and ϵ), the CO vibrational frequency shifts linearly. Also, an electric field perturbation was applied to the system by introducing a quantity V_E to the interaction potential, where V_E is given by

$$V_E = E_z(du/dz)(z° - z) \quad (28)$$

where E_z is the electric field strength in the z direction (normal to the electrode surface), du/dz is obtained from expansion of the dipole moment function, and ($z°$ – z) is the relative displacement from the equilibrium position $z°$. This type of potential is consistent with the Gouy–Chapman model of the electrochemical double layer. The experimental value of du/dz for gas-phase CO has been reported;[178] Lambert has determined that the value for adsorbed CO is about twice that of the gas-phase species.[81] With this observation, a Stark tuning rate was calculated that was in excellent agreement with Lambert's value. The calculated CO stretching frequency was also found to be linearly dependent on the electric field strength.[82]

It should be pointed out that other potential energy surfaces describing the interaction of adsorbed species on metal surfaces have been derived by using other potential energy functions.[78,179,180] Tully[181] has constructed potential energy surfaces for CO(ads) on Pt(111) for the purpose of studying gas-phase dynamics.

Since the electric field depends upon the accumulation of charge on the electrode surface, it is difficult to separate electric field perturbations from changes in bonding between the adsorbate and the metal. It is probable that experimentally observed spectral shifts are due to a combination of chemical bonding and electric field interactions.

The above model has also been applied to the analysis of the vibrational frequencies of ferro- and ferricyanide adsorbed on metal electrodes.[182] We know that the rate of electron transfer of this redox couple is dependent on the electrode material as well as the nature and concentration of cation species in solution.[183,184] Several models have been suggested in efforts to explain the kinetic behavior at the electrode surface. Schleinitz et al.[183] proposed formation of a dimeric species in which a cation bridge is formed between the reacting species. Sohr and co-workers[184] proposed a similar model, which involved stabilization by the surface.

Many studies have indicated ferricyanide and ferrocyanide adsorption, including radiotracer methods,[74] in situ vibrational spectroscopic methods,[76] and SERS studies.[75,185]

A potential energy function was constructed to describe the interactions of ferri- and ferrocyanide with a metal electrode surface[182] in a similar manner to that for CO adsorbed on platinum.[82] Again, the vibrational frequencies of the adsorbed iron species were calculated by expansion of the potential function to second order using the Cartesian form of the Taylor series. It was determined that the vibrational frequencies are dependent on the electrode-adsorbate orientation and binding energy and that ion pairing with alkali metal cations has only a minimal effect on the vibrational frequencies. However, it was suggested that ion-pairing interactions may be important in stabilizing adsorbate-surface orientations. Computed vibrational frequencies for this system compared favorably with SERS and in situ infrared spectra.

Calculations of surface metal atom and adsorbate vibrations using cluster models have been successful in describing the dynamics of many of these systems.[89,172,180,187] The far-infrared spectra of lithium deposited on a gold electrode[150] have been interpreted by using a cluster model.[188] The model was used to calculate Li surface atom vibrations, assuming central forces between all atoms of the cluster. Using a Morse potential energy function, the cluster model was used to predict the far-infrared spectrum of lithium on Au(111). Excellent agreement with experiment was reported for calculations involving one and two layers of lithium on the gold surface.

Acknowledgments. We thank the Office of Naval Research for support of this work.

References

(1) (a) Rosasco, S. D.; Stickney, J. L.; Salaita, G. N.; Frank, D. G.; Katekaru, J. Y.; Schardt, B. C.; Soriaga, M. P.; Stern, D.

A.; Hubbard, A. T. *J. Electroanal. Chem.* **1985**, *188*, 95. (b) Schardt, B. C.; Stickney, J. L.; Stern, D. A.; Wieckowski, A.; Zapien, D. C.; Hubbard, A. T. *Langmuir* **1987**, *3*, 239. (c) Harrington, D. A.; Wieckowski, A.; Rosasco, S. D.; Salaita, G. N.; Hubbard, A. T. *Langmuir* **1985**, *1*, 232. (d) Salaita, G. N.; Stern, D. A.; Lu, F.; Baltruschadt, H.; Schardt, B. C.; Stickney, J. L.; Soriaga, M. P.; Frank, D. G.; Hubbard, A. T. *Langmuir* **1986**, *2*, 828.
(2) Bellier, J. P.; Lecoeur, J.; Rousseau, A. *J. Electroanal. Chem.* **1986**, *200*, 55.
(3) (a) Peukert, M.; Ibach, H. *Surf. Sci.* **1984**, *136*, 319. (b) Sexton, B. A. *Appl. Phys.* **1981**, *A26*, 1.
(4) Mark, H. B., Jr.; Pons, S. *Anal. Chem.* **1966**, *38*, 119.
(5) (a) Reed, A. H.; Yeager, E. *Electrochim. Acta* **1970**, *15*, 1345. (b) Reed, A. H.; Yeager, E. *Appl. Opt.* **1968**, *7*, 451.
(6) Tallant, D.; Evans, D. H. *Anal. Chem.* **1969**, *41*, 835.
(7) Fleischmann, M.; Hendra, P. J.; McQuillann, A. J. *J. Chem. Soc., Chem. Commun.* **1973**, 80.
(8) (a) Fleischmann, M.; Hill, I. R. In *Electrochemical Effects in Surface Enhanced Raman Scattering*; Chang, R. K., Furtak, T. E., Eds.; Plenum: New York, 1982. (b) Cooney, R. P.; Mahoney, M. R.; McQuillan, A. J. In *Advances in Infrared and Raman Spectroscopy*; Clark, R. J. H., Hester, R. E., Eds.; Heyden: London, 1982; Vol. 9.
(9) (a) Bewick, A.; Kunimatsu, K.; Pons, S. *Electrochim. Acta* **1980**, *25*, 465. (b) Pons, S. Ph.D. Dissertation, University of Southampton, England, 1979. (c) Bewick, A.; Kunimatsu, K. *Surf. Sci.* **1980**, *101*, 131.
(10) (a) Bewick, A.; Robinson, J. *J. Electroanal. Chem.* **1975**, *60*, 163. (b) Bewick, A.; Robinson, J. *Surf. Sci.* **1976**, *55*, 349. (c) Bewick, A.; Mellor, J. M.; Pons, S. *Electrochim. Acta* **1980**, *25*, 931.
(11) Adžić, R.; Cahan, B. D.; Yeager, E. *J. Chem. Phys.* **1975**, *60*, 163.
(12) Aylmer-Kelly, A. W.; Bewick, A.; Cantrell, P. R.; Tuxford, A. M. *Discuss. Faraday Soc.* **1973**, *56*, 96.
(13) Bewick, A.; Edwards, G. J.; Mellor, J. M.; Pons, S. *J. Chem. Soc., Perkin Trans. 2* **1977**, 1952.
(14) Ashley, K.; Pons, S. *Trends Anal. Chem.* **1986**, *5*, 263.
(15) (a) Otto, A. *Surf. Sci.* **1980**, *101*, 99. (b) Kolb, D. M.; Kötz, R.; Yamamoto, K. *Surf. Sci.* **1979**, *87*, 20. (c) Kolb, D. M. In *Surface Polaritons*; Agronovich, V. M., Mills, D. L., Eds.; Elsevier North-Holland: New York, 1982.
(16) Clarke, J. S.; Kuhn, A. T.; Orville-Thomas, W. J.; Stedman, M. *J. Electroanal. Chem.* **1974**, *49*, 199.
(17) Bewick, A. Paper presented at The Electrochemical Society Meeting, Montreal, 1982.
(18) Pons, S.; Bewick, A. *Nav. Res. Rev.* **1985**, *37*, 33 and references therein.
(19) Golden, W. G.; Dunn, D. S.; Overend, J. *J. Catal.* **1981**, *71*, 395.
(20) Golden, W. G.; Saperstein, D.; Severson, M. W.; Overend, J. *J. Phys. Chem.* **1984**, *88*, 874.
(21) (a) Russell, J. W.; Overend, J.; Scanlon, K.; Severson, M.; Bewick, A. *J. Phys. Chem.* **1982**, *86*, 3066. (b) Russell, J. W.; Severson, M.; Scanlon, K.; Overend, J.; Bewick, A. *J. Phys. Chem.* **1982**, *87*, 293.
(22) Golden, W. G.; Kunimatsu, K.; Seki, H. *J. Phys. Chem.* **1984**, *88*, 1275.
(23) Kunimatsu, K.; Seki, H.; Golden, W. G. *Chem. Phys. Lett.* **1985**, *108*, 195.
(24) (a) Foley, J. K.; Korzeniewski, C.; Daschbach, J. L.; Pons, S. In *Electroanalytical Chemistry*; Bard, A. J., Ed.; Marcel Dekker: New York, 1986; Vol. 14. (b) Bewick, A.; Pons, S. In *Advances in Infrared and Raman Spectroscopy*; Clark, R. J. H., Hester, R. E., Eds.; Heyden: London, 1985; Vol. 12. (c) Ashley, K.; Pons, S. *Trends Anal. Chem.* **1985**, *4*, 142. (d) Foley, J. K.; Pons, S. *Anal. Chem.* **1985**, *57*, 945A. (e) Pons, S.; Foley, J. K.; Russell, J. W.; Severson, M. In *Modern Aspects of Electrochemistry*; Bockris, J. O'M., Conway, B. E., Eds.; Plenum: New York, 1986. (f) Korzeniewski, C.; Pons, S. *Prog. Anal. Spectrosc.* **1987**, *10*, 1. (g) Korzeniewski, C.; Foley, J. K.; Pons, S. *Indian J. Technol.* **1986**, *24*, 347.
(25) Hecht, E.; Zajac, A. *Optics*; Addison-Wesley: Reading, MA, 1974.
(26) Greenler, R. G. *J. Chem. Phys.* **1966**, *44*, 310.
(27) Bewick, A.; Kunimatsu, K.; Pons, S.; Russell, J. W. *J. Electroanal. Chem.* **1984**, *160*, 47. Kunimatsu, K. *J. Electroanal. Chem.* **1982**, *140*, 205.
(28) Hipps, K. W.; Crosby, G. A. *J. Phys. Chem.* **1979**, *83*, 555.
(29) Bradshaw, A. M.; Hoffman, T. *Surf. Sci.* **1975**, *52*, 449.
(30) (a) Golden, W. G.; Saperstein, D. *J. Electron Spectrosc.* **1983**, *30*, 43. (b) Golden, W. G.; Kunimatsu, K.; Seki, H. *J. Phys. Chem.* **1984**, *88*, 1275.
(31) Dowrey, A. E.; Marcott, C. *Appl. Spectrosc.* **1982**, *36*, 414.
(32) Seki, H.; Kunimatsu, K.; Golden, W. G. *Appl. Spectrosc.* **1985**, *39*, 437.
(33) (a) Neugebauer, G.; Nauer, N.; Brinda-Konopik, N.; Kellner, R. *Z. Anal. Chem.* **1983**, *314*, 266. (b) Neugebauer, G.; Nekel, A.; Nauer, G.; Brinda-Konopik, N.; Garnier, F.; Tourillon, G. *J. Phys. (Paris)* **1983**, *C44*, 517. (c) Neugebauer, G.; Nauer, N.; Brinda-Konopik, N.; Gidaly, G. *J. Electroanal. Chem.* **1981**, *122*, 381.
(34) Pons, S. *J. Electroanal. Chem.* **1983**, *150*, 495.
(35) Corrigan, D. S.; Weaver, M. J. *Rev. Sci. Instrum.* **1985**, *56*, 1665.
(36) Dignam, M. J.; Baker, M. D. *J. Vac. Sci. Technol.* **1982**, *21*, 80.
(37) (a) Bockris, J. O'M.; Reddy, A. K. N. *Modern Electrochemistry*; Plenum: New York, 1973; Vol. 2, Chapter 7. (b) Bard, A. J.; Faulkner, L. R. *Electrochemical Methods*; Wiley: New York, 1980; Chapter 12.
(38) (a) Korzeniewski, C.; Shirts, R. B.; Pons, S. *J. Phys. Chem.* **1985**, *89*, 2297. (b) Korzeniewski, C. Ph.D. Dissertation, University of Utah, 1987.
(39) Sass, J. K.; Neff, H.; Moskovits, M.; Holloway, S. *J. Phys. Chem.* **1981**, *85*, 621.
(40) Bewick, A.; Russell, J. W. *J. Electroanal. Chem.* **1982**, *132*, 329.
(41) Bewick, A.; Russell, J. W. *J. Electroanal. Chem.* **1982**, *142*, 337. Nichols, R. J.; Bewick, A., submitted for publication.
(42) Kyriacau, D. K.; Jannakoudakis, D. A. *Electrocatalysis for Organic Synthesis*; Wiley: New York, 1986.
(43) Capon, A.; Parsons, R. *J. Electroanal. Chem.* **1973**, *44*, 1.
(44) McNicol, B. D. *J. Electroanal. Chem.* **1981**, *118*, 71.
(45) Breiter, M. W. In *Modern Aspects of Electrochemistry*; Bockris, J. O'M., Conway, B. E., Eds.; Plenum: Ew York, 1970; Vol. 10.
(46) Clavilier, J.; Sun, S. G. *J. Electroanal. Chem.* **1986**, *199*, 471.
(47) Breiter, M. W. *J. Electroanal. Chem.* **1967**, *14*, 406.
(48) Biegler, T. *Aust. J. Chem.* **1969**, *22*, 1583.
(49) (a) Sobkowski, J.; Wieckowski, A. *J. Electroanal. Chem.* **1972**, *34*, 185. (b) Sobkowski, J.; Wieckowski, A. *J. Electroanal. Chem.* **1975**, *63*, 365.
(50) Allen, G. C.; Tucker, P. M.; Capon, A.; Parsons, R. *J. Electroanal. Chem.* **1974**, *50*, 335.
(51) Beden, B.; Lamy, C.; Bewick, A.; Kunimatsu, K. *J. Electroanal. Chem.* **1981**, *121*, 343.
(52) Juanto, S.; Beden, B.; Hahn, F.; Leger, J.-M.; Lamy, C. *J. Electroanal. Chem.*, in press.
(53) Beden, B.; Juanto, S.; Leger, J.-M.; Lamy, C. *J. Electroanal. Chem.*, in press.
(54) Beden, B.; Bewick, A.; Lamy, C. *J. Electroanal. Chem.* **1983**, *148*, 147.
(55) Kunimatsu, K. *J. Electroanal. Chem.* **1986**, *213*, 149.
(56) Bewick, A.; Kunimatsu, K.; Beden, B.; Lamy, C. 32nd ISE Meeting, Dubrovnik, Yugoslavia, 1981, Abstract A28.
(57) Sun, S. G.; Clavilier, J.; Bewick, A. *J. Electroanal. Chem.*, in press.
(58) Hahn, F.; Beden, B.; Lamy, C. *J. Electroanal. Chem.* **1986**, *204*, 315.
(59) Foley, J. K. M.Sc. Thesis, University of Southampton, England, 1982.
(60) Hahn, F.; Beden, B.; Kadirgan, F.; Lamy, C. *J. Electroanal. Chem.* **1987**, *216*, 169.
(61) Sheppard, N.; Nguyen, T. T. In *Advances in Infrared and Raman Spectroscopy*; Clark, R. J. H., Hester, R. E., Eds.; Heyden: London, 1978; Vol. 5.
(62) Beden, B.; Bewick, A.; Kunimatsu, K.; Lamy, C. *J. Electroanal. Chem.* **1982**, *142*, 345.
(63) Kunimatsu, K.; Golden, W. G.; Seki, H.; Philpott, M. R. *Langmuir* **1985**, *1*, 245.
(64) Kunimatsu, K.; Seki, H.; Golden, W. G.; Gordon, J. G., II; Philpott, M. R. *Surf. Sci.* **1985**, *158*, 586.
(65) Pham, M.-C.; Adami, F.; Laçaze, P.-C.; Doucet, J.-P.; Dubois, J.-E. *J. Electroanal. Chem.* **1986**, *201*, 413.
(66) Kunimatsu, K.; Kita, H. *J. Electroanal. Chem.* **1987**, *218*, 155.
(67) Bewick, A.; Beden, B.; Razaq, M.; Weber, J. *J. Electroanal. Chem.* **1982**, *139*, 209.
(68) Spasojevic, M.; Adžić, R. R.; Despic, A. R. *J. Electroanal. Chem.* **1980**, *109*, 261.
(69) Avramov-Ivic, M.; Adžić, R. R.; Bewick, A.; Razaq, M. *J. Electroanal. Chem.*, in press.
(70) (a) Sibille, S.; Moiroux, J.; Marot, J. C. *J. Electroanal. Chem.* **1978**, *88*, 105. (b) Fleury, M. B.; Lettelier, S.; Dufresne, J. S.; Moiroux, J. *J. Electroanal. Chem.* **1978**, *88*, 123.
(71) Kuta, J.; Yeager, E. *J. Electroanal. Chem.* **1975**, *59*, 110.
(72) Peter, L. M.; Durr, W.; Bindra, P.; Gerischer, H. *J. Electroanal. Chem.* **1983**, *145*, 163.
(73) Kawiak, J.; Jedral, T.; Galus, Z. *J. Electroanal. Chem.* **1983**, *145*, 163.
(74) Wieckowski, A.; Szklarcyk, M. *J. Electroanal. Chem.* **1982**, *142*, 157.
(75) Fleischmann, M.; Graves, P. R.; Robinson, J. *J. Electroanal. Chem.* **1985**, *182*, 87.
(76) Pons, S.; Datta, M.; McAleer, J. F.; Hinman, A. S. *J. Electroanal. Chem.* **1984**, *160*, 369.
(77) Korzeniewski, C.; McKenna, W. P.; Pons, S., submitted.

(78) Ray, N. K.; Anderson, A. B. *J. Phys. Chem.* **1982**, *86*, 4851.
(79) Anderson, A. B.; Kötz, R.; Yeager, E. *Chem. Phys. Lett.* **1981**, *82*, 130.
(80) Holloway, S.; Norskov, J. K. *J. Electroanal. Chem.* **1984**, *161*, 193.
(81) Lambert, D. *Solid State Commun.* **1984**, *51*, 197.
(82) Korzeniewski, C.; Pons, S.; Schmidt, P. P.; Severson, M. W. *J. Chem. Phys.* **1986**, *85*, 4153.
(83) Krebs, H. J.; Luth, H. *Appl. Phys.* **1977**, *14*, 337.
(84) Baker, M. D.; Chester, M. A. In *Vibrations at Surfaces*; Caudano, R., Gilles, J. M., Lucas, A. A., Eds.; Plenum: New York, 1982.
(85) Severson, M. W.; Tornquist, W. J.; Overend, J. *J. Phys. Chem.* **1984**, *88*, 469.
(86) Severson, M. W.; Russell, A.; Campbell, D.; Russell, J. W. *Langmuir* **1987**, *3*, 202.
(87) Beden, B.; Collas, N.; Lamy, C.; Leger, J. M.; Solis, V. *Surf. Sci.* **1985**, *162*, 789.
(88) Kunimatsu, K.; Seki, H.; Golden, W. G.; Gordon, J. G., II; Philpott, M. R. *Langmuir* **1986**, *2*, 464.
(89) Bagus, P. S.; Müller, W. *Chem. Phys. Lett.* **1985**, *115*, 540.
(90) Kunimatsu, K.; Aramata, A.; Nakajima, H.; Kita, H. *J. Electroanal. Chem.* **1986**, *207*, 293.
(91) Tornquist, W. J.; Guillaume, F.; Griffin, G. L. *Langmuir*, in press.
(92) Nakajima, H.; Kita, H.; Kunimatsu, K.; Aramata, A. *J. Electroanal. Chem.* **1986**, *201*, 175.
(93) Ikezawa, Y.; Saito, H.; Yamazaki, M.; Toda, G. *J. Electroanal. Chem.*, in press.
(94) Pons, S.; Bewick, A. *Langmuir* **1985**, *1*, 141.
(95) Hubbard, A. T.; Stickney, J.; Soriaga, M. P.; Chia, V.; Rosasco, S.; Schardt, B.; Solomun, T.; Song, D.; White, J.; Wieckowski, A. *J. Electroanal. Chem.* **1984**, *168*, 43.
(96) Foley, J. K. Ph.D. Dissertation, University of Utah, 1986.
(97) Corrigan, D. S.; Gao, P.; Leung, L.-W. H.; Weaver, M. J. *Langmuir* **1986**, *2*, 744.
(98) Gao, P.; Weaver, M. J. *J. Phys. Chem.* **1985**, *89*, 5040.
(99) Korzeniewski, C.; Pons, S. *Langmuir* **1986**, *2*, 468.
(100) Korzeniewski, C.; Pons, S. *J. Vac. Sci. Technol. B* **1985**, *3*, 1421.
(101) Soriaga, M. P.; Binamira-Soriaga, E.; Hubbard, A. T.; Benziger, J. B.; Pang, K.-W. P. *Inorg. Chem.* **1985**, *24*, 65.
(102) Bree, A.; Kydd, R. A.; Misra, T. N.; Vilkos, V. V. B. *Spectrochim. Acta, Part A* **1971**, *27*, 2315.
(103) Solomun, T. *J. Electroanal. Chem.* **1986**, *199*, 443.
(104) Kunimatsu, K.; Bewick, A. *Indian J. Technol.* **1986**, *24*, 407.
(105) Beden, B.; Morin, M.-C.; Hahn, F.; Lamy, C. *J. Electroanal. Chem.* **1987**, *229*, 353.
(106) Kunimatsu, K.; Seki, H.; Golden, W. G.; Gordon, J. G., II; Philpott, M. R. *Langmuir*, in press.
(107) Bewick, A.; Gibilaro, C., submitted.
(108) (a) Otto, A. *Surf. Sci.* **1978**, *75*, L392. (b) Otto, A. *Surf. Sci.* **1980**, *92*, 145. (c) Billman, J.; Kovacs, G.; Otto, A. *Surf. Sci.* **1980**, *92*, 153. (d) Timper, J.; Billman, J.; Otto, A.; Pockrand, I. B. *Surf. Sci.* **1980**, *101*, 348.
(109) (a) Furtak, T. E.; Trott, G.; Loo, B. H. *Surf. Sci.* **1980**, *101*, 374. (b) Furtak, T. E. *Solid State Commun.* **1978**, *28*, 903. (c) Loo, B. H.; Furtak, T. E. *Chem. Phys. Lett.* **1980**, *71*, 68.
(110) (a) Dornhous, R.; Long, M. B.; Benner, R. E.; Chang, R. K. *Surf. Sci.* **1980**, *93*, 240. (b) Benner, R. E.; Dornhous, R.; Chang, R. K.; Laube, B. L. *Surf. Sci.* **1980**, *101*, 341. (c) Chen, T. K.; von Raben, K. V.; Murphy, D. V.; Chang, R. K.; Laube, B. L. *Surf. Sci.* **1984**, *143*, 169.
(111) Kötz, R.; Yeager, E. *J. Electroanal. Chem.* **1981**, *123*, 335.
(112) Genack, A. Z.; Weitz, D. A.; Granila, T. J. *Surf. Sci.* **1980**, *101*, 381.
(113) Fleischmann, M.; Hendra, P. J.; Hill, I. R.; Pemble, M. *J. Electroanal. Chem.* **1981**, *117*, 243. (b) Fleischmann, M.; Hill, I. R. *J. Electroanal. Chem.* **1983**, *146*, 369. (c) Fleischmann, M.; Sundholm, G.; Tian, Z. Q. *Electrochim. Acta* **1986**, *31*, 907. (d) Fleischmann, M.; Tian, Z. Q. *J. Electroanal. Chem.* **1987**, *217*, 385. (e) Fleischmann, M.; Tian, Z. Q.; Li, L. J. *J. Electroanal. Chem.* **1987**, *217*, 397. (f) Fleischmann, M.; Tian, Z. Q. *J. Electroanal. Chem.* **1987**, *217*, 411.
(114) (a) Wetzel, H.; Gerischer, H.; Pettinger, B. *Chem. Phys. Lett.* **1981**, *78*, 392. (b) Pettinger, B.; Philpott, M. R.; Gordon, J. G., II. *Surf. Sci.* **1981**, *104*, 934. (c) Pettinger, B.; Philpott, M. R.; Gordon, J. G., II. *Surf. Sci.* **1981**, *105*, 469. (d) Weaver, M. J.; Hupp, J. T.; Barz, F.; Gordon, J. G., II; Philpott, M. R. *J. Electroanal. Chem.* **1984**, *160*, 321.
(115) (a) Fleischmann, M.; Hendra, P. J.; Hill, I. R.; Pemble, M. *J. Electroanal. Chem.* **1981**, *117*, 243. (b) Fleischmann, M.; Hill, I. R. *J. Electroanal. Chem.* **1983**, *146*, 369. (c) Fleischmann, M.; Sundholm, G.; Tian, Z. Q. *Electrochim. Acta* **1986**, *31*, 907. (d) Fleischmann, M.; Tian, Z. Q. *J. Electroanal. Chem.* **1987**, *217*, 385. (e) Fleischmann, M.; Tian, Z. Q.; Li, L. J. *J. Electroanal. Chem.* **1987**, *217*, 397. (f) Fleischmann, M.; Tian, Z. Q. *J. Electroanal. Chem.* **1987**, *217*, 411.
(116) (a) Wetzel, H.; Gerischer, H.; Pettinger, B. *Chem. Phys. Lett.* **1981**, *78*, 392. (b) Pettinger, B.; Philpott, M. R.; Gordon, J. G., II. *Surf. Sci.* **1981**, *104*, 934. (c) Pettinger, B.; Philpott, M. R.; Gordon, J. G., II. *Surf. Sci.* **1981**, *105*, 469. (d) Weaver, M. J.; Hupp, J. T.; Barz, F.; Gordon, J. G., II; Philpott, M. R. *J. Electroanal. Chem.* **1984**, *160*, 321.
(117) Hatta, A.; Sasaki, Y.; Suëtaka, W. *J. Electroanal. Chem.* **1986**, *215*, 93.
(118) Kretschmann, E. *Z. Phys.* **1971**, *241*, 313.
(119) Wetzel, H.; Gerischer, H.; Pettinger, B. *Chem. Phys. Lett.* **1981**, *80*, 159.
(120) (a) Neff, H.; Lange, P.; Roe, D. K.; Sass, J. K. *J. Electroanal. Chem.* **1983**, *150*, 513. (b) Lange, P.; Glaw, V.; Neff, H.; Piltz, E.; Sass, J. K. *Vacuum* **1983**, *33*, 763.
(121) Benziger, J. B.; Pascal, F. A.; Bernasek, S. L.; Soriaga, M. P.; Hubbard, A. T. *J. Electroanal. Chem.* **1986**, *198*, 65.
(122) (a) Cooney, R. P.; Reid, E. S.; Fleischmann, M.; Hendra, P. J. *J. Chem. Soc., Faraday Trans. 1* **1977**, *73*, 1691. (b) Gold, H. S.; Buck, R. P. *J. Raman Spectrosc.* **1979**, *8*, 323.
(123) Corrigan, D. S.; Foley, J. K.; Gao, P.; Pons, S.; Weaver, M. J. *Langmuir* **1985**, *1*, 616.
(124) Foley, J. K.; Pons, S.; Smith, J. J. *Langmuir* **1985**, *1*, 697.
(125) Corrigan, D. S.; Weaver, M. J. *J. Phys. Chem.* **1986**, *90*, 5300.
(126) Bewick, A. In *Proc. Symp. Chem. Phys. Electrocatal.*, The Electrochemical Society Meeting, San Francisco, 1983.
(127) Bockris, J. O'M.; Reddy, A. K. N. *Modern Electrochemistry*; Plenum: New York, 1970; Vol. 1.
(128) Pons, S.; Davidson, T.; Bewick, A. *J. Electroanal. Chem.* **1981**, *125*, 237.
(129) (a) Saumagne, P. Thèse de Docteur, Université de Bordeaux, France, 1981. (b) Saumagne, P.; Josien, M. L. *Bull. Soc. Chim. Fr.* **1985**, 813. (c) Gentric, E. Thèse de Docteur, Université de Bretagne Occidentale, France, 1972.
(130) Foley, J. K.; Korzeniewski, C.; Pons, S., submitted.
(131) Corrigan, D. S.; Weaver, M. J., submitted.
(132) (a) Baizer, M.; Lund, H., Eds. *Organic Electrochemistry*, 2nd ed.; Marcel Dekker: New York, 1983. (b) Weinberg, N. L., Ed. *Technique of Electroorganic Synthesis*; Wiley: New York, 1975; Part II. (c) Ross, S. D.; Finkelstein, M.; Rudd, E. F. *Anodic Oxidation*; Academic: New York, 1975. (d) Yoshida, K. *Electrooxidation in Organic Chemistry*; Wiley: New York, 1984.
(133) (a) Winograd, N.; Blount, H. N.; Kuwana, T. *J. Phys. Chem.* **1969**, *73*, 3456. (b) Kuwana, T. *Ber. Bunsenges Phys. Chem.* **1973**, *77*, 858. (c) Kuwana, T.; Heineman, W. R. *Acc. Chem. Res.* **1976**, *9*, 241. (d) Heineman, W. R.; Hawkridge, F. M.; Blount, H. N. In New York, 1984, Vol. 13, Chapter 1.
(134) (a) Khoo, S. B. Ph.D. Dissertation, University of Alberta, Canada, 1984. (b) Khoo, S. B.; Foley, J. K.; Pons, S. *J. Electroanal. Chem.* **1987**, *218*, 254.
(135) Ashley, K. Ph.D. Dissertation, University of Utah, 1987.
(136) Khoo, S. B.; Foley, J. K.; Korzeniewski, C.; Pons, S.; Marcott, C. *J. Phys. Chem.*, in press.
(137) (a) Khatkale, M. S.; Devlin, J. P. *J. Phys. Chem.* **1979**, *83*, 1637. (b) Moore, J. C.; Smith, D.; Younhe, Y.; Devlin, J. P. *J. Phys. Chem.* **1971**, *75*, 325. (c) Hinckley, J. J.; Devlin, J. P. *J. Chem. Phys.* **1973**, *58*, 4750.
(138) Penfold, B. R.; Lipscomb, W. N. *Acta Crystallogr.* **1961**, *14*, 589.
(139) (a) Jeanmaire, D. L.; Suchanski, M. R.; Van Duyne, R. P. *J. Am. Chem. Soc.* **1975**, *97*, 1699. (b) Pemberton, J. E.; Buck, R. P. *Appl. Spectrosc.* **1981**, *35*, 571.
(140) Stanley, J.; Smith, D.; Latimer, B.; Devlin, J. P. *J. Phys. Chem.* **1966**, *70*, 2011.
(141) (a) Itoh, M. *Bull. Chem. Soc. Jpn.* **1972**, *65*, 1947. (b) Yokoyama, K.; Maeda, S.; Etoh, C.; Matsuzaki, S.; Toyoda, K. *Bull. Chem. Soc. Jpn.* **1980**, *53*, 36. (c) Matsuzaki, S.; Mitsubishi, T.; Toyoda, K. *Chem. Phys. Lett.* **1982**, *91*, 296.
(142) Pons, S.; Davidson, T.; Bewick, A. *J. Am. Chem. Soc.* **1982**, *105*, 1802.
(143) Juchnovski, I. *Spectrochim. Acta* **1973**, *29*, 1273.
(144) Aleksandrov, I. V.; Bobovich, Y. S.; Maslovad, V. G.; Sidorov, A. N. *Opt. Spectrosc.* **1973**, *35*, 154.
(145) Blackwood, D. J.; Pons, S., submitted.
(146) Daschbach, J. L.; Heisler, D.; Pons, S. *Appl. Spectrosc.* **1986**, *40*, 489.
(147) Li, J.; Daschbach, J. L.; Smith, J. J.; Morse, M. D.; Pons, S. *J. Electroanal. Chem.* **1986**, *209*, 387.
(148) Roe, D. K.; Sass, J. K.; Bethune, D. S.; Luntz, A. C. *J. Electroanal. Chem.* **1987**, *216*, 293.
(149) Yaniger, S. I.; Vidrine, D. W. *Appl. Spectrosc.* **1986**, *41*, 174.
(150) Li, J.; Pons, S.; Smith, J. J. *Langmuir* **1986**, *2*, 297.
(151) Habib, M. A.; Bockris, J. O'M. *J. Electrochem. Soc.* **1983**, *130*, 2510.
(152) Zelaney, P.; Habib, M. A.; Bockris, J. O'M. *J. Electrochim. Soc.* **1984**, *131*, 2465.
(153) Bockris, J. O'M.; Habib, M. A.; Carbejal, J. L. *J. Electrochem. Soc.* **1984**, *131*, 3032.
(154) Habib, M. A.; Bockris, J. O'M. *J. Electrochem. Soc.* **1985**, *132*, 108.
(155) Aurian-Blajeni, B. A.; Habib, M. A.; Taniguchi, I.; Bockris, J. O'M. *J. Electrochem. Soc.* **1983**, *157*, 399.

(156) Chandrasekaran, K.; Bockris, J. O'M. *Surf. Sci.* **1986**, *175*, 623.
(157) Venkateswara Rao, A.; Chazalviel, J.-N.; Ozanam, F. *J. Appl. Phys.* **1986**, *60*, 696.
(158) Chazalviel, J.-N.; Venkateswara Rao, A. *J. Electrochem. Soc.* **1987**, *134*, 1138.
(159) Chazalviel, J.-N. *J. Electroanal. Chem.*, in press.
(160) Venkateswara Rao, A.; Chazalviel, J.-N. *J. Electrochem. Soc.*, in press.
(161) (a) Harrick, N. J. *Phys. Rev.* **1962**, *25*, 1165. (b) Harrick, N. J.; Beckman, K. H. In *Characterization of Solid Surfaces*; Kane, P. F., Larrabee, G. R., Eds.; Plenum: New York, 1974; Chapter 10.
(162) Lucovsky, G. *Solid State Commun.* **1965**, *3*, 299.
(163) Li, J.; Pons, S., submitted.
(164) Datta, M.; Freeman, J. J.; Janssen, E. W. *Spectrosc. Lett.* **1985**, *18*, 273.
(165) Nakamoto, N. In *Infrared and Raman Spectra of Inorganic and Coordination Compounds*, 3rd ed.; Wiley: New York, 1978.
(166) Allara, D. L.; Nuzzo, R. G. *Langmuir* **1985**, *1*, 52.
(167) Marcott, C. *Appl. Spectrosc.* **1984**, *38*, 442.
(168) Crumbliss, A. L.; Lugg, P. S.; Childers, W.; Palmer, R. A. *J. Phys. Chem.* **1985**, *89*, 482.
(169) Niwa, K.; Doblhofer, K. *Electrochim. Acta* **1986**, *31*, 439.
(170) Nazri, G.; Corrigan, D. A.; Maheswari, S. P. *Langmuir*, in press.
(171) Bagus, P. S.; Bauschlincher, C. W., Jr.; Nelin, C. J.; Laskowski, B. C.; Seel, M. *J. Chem. Phys.* **1984**, *81*, 3594.
(172) Muetterties, E. L.; Rhodin, T. N.; Band, E.; Brucker, C. F.; Pretzer, W. R. *Chem. Rev.* **1979**, *79*, 91.
(173) (a) Schmidt, P. P.; Pons, S.; McKinley, J. M. *J. Chem. Soc., Faraday Trans. 2* **1980**, *76*, 979. (b) McKinley, J. M.; Schmidt, P. P. *J. Chem. Soc., Faraday Trans. 2* **1982**, *78*, 867. (c) McKinley, J. M.; Schmidt, P. P. *Chem. Phys. Lett.* **1984**, *110*, 379.
(174) (a) Schmidt, P. P.; Pons, S. *Electrochim. Acta* **1982**, *27*, 867. (b) Schmidt, P. P.; Pons, S. *Electrochim. Acta* **1982**, *27*, 875.
(175) (a) Schmidt, P. P. *J. Chem. Soc., Faraday Trans. 2* **1982**, *78*, 123. (b) Schmidt, P. P. *J. Chem. Soc., Faraday Trans. 2* **1984**, *80*, 157. (c) Schmidt, P. P. *J. Chem. Soc., Faraday Trans. 2* **1984**, *80*, 181. (d) Schmidt, P. P. *J. Chem. Soc., Faraday Trans. 2* **1985**, *81*, 341. (e) Schmidt, P. P. *J. Chem. Soc., Faraday Trans. 2* **1986**, *82*, 1399.
(176) (a) Chang, S. S.; Severson, M. W.; Schmidt, P. P. *J. Phys. Chem.* **1985**, *89*, 2892. (b) Chang, S. S.; Schmidt, P. P.; Severson, M. W. *J. Phys. Chem.* **1986**, *90*, 1046. (c) Schmidt, P. P.; Chang, S. S. *J. Phys. Chem.*, in press.
(177) Rose, M. E. *Elementary Theory of Angular Momentum*; Wiley: New York, 1957.
(178) Bouanich, J.-P.; Brodbeck, C. *J. Quant. Spectrosc. Radiat. Transfer* **1974**, *14*, 119.
(179) Fink, W. H.; Banerjee, A.; Simons, J. *J. Chem. Phys.* **1983**, *79*, 6104.
(180) Avouris, Ph.; Bagus, P. S.; Rossi, A. R. *J. Vac. Sci. Technol. B* **1985**, *3*, 1484.
(181) Tully, J. C. *J. Chem. Phys.* **1980**, *73*, 6333.
(182) Korzeniewski, C.; Severson, M. W.; Schmidt, P. P.; Pons, S.; Fleischmann, M. *J. Phys. Chem.*, in press.
(183) (a) Schleinitz, K. D.; Landsberg, R.; Lowis von Menar, G. V. *J. Electroanal. Chem.* **1970**, *28*, 279. (b) Schleinitz, K. D.; Landsberg, R.; Lowis von Menar, G. V. *J. Electroanal. Chem.* **1970**, *28*, 287.
(184) (a) Sohr, R.; Müller, L.; Landsberg, R. *J. Electroanal. Chem.* **1974**, *50*, 55. (b) Sohr, R.; Müller, L. *Electrochim. Acta* **1975**, *20*, 451.
(185) Weaver, M. J.; Gao, P.; Gosztola, D.; Patterson, M. L.; Tadayyoni, M. A. in *Excited States and Reaction Intermediates*; ACS Symposium Series 307; American Chemical Society: Washington, DC, 1986; p 4153.
(186) Califano, S. *Vibrational States*; Wiley: New York, 1976.
(187) (a) Lloyd, K. G.; Hemminger, J. C. *J. Chem. Phys.* **1985**, *82*, 3858. (b) Ariyasu, J. C.; Mills, D. L.; Lloyd, K. G.; Hemminger, J. C. *Phys. Rev. B* **1984**, *30*, 507.
(188) Severson, M. W.; Pons, S.; Schmidt, P. P.; Li, J.; Smith, J. J. *Phys. Rev. B*, in press.
(189) (a) Ozanam, F.; Chazalviel, J.-N. *J. Electron. Spectrosc.*, in press. (b) Ozanam, F.; Chazalviel, J.-N. *Rev. Sci. Instrum.*, in press.